NOAA Technical Report ERL 384-PMEL 27

A General Model of the Ocean Mixed Layer

Using a Two-Component Turbulent Kinetic Energy Budget with Mean Turbulent Field Closure

Roland W. Garwood, Jr.

Pacific Marine Environmental Laboratory
Seattle, Washington

September 1976

U.S. DEPARTMENT OF COMMERCE
Elliot Richardson, Secretary

National Oceanic and Atmospheric Administration
Robert M. White, Administrator

Environmental Research Laboratories
Wilmot Hess, Director

Boulder, Colorado

Adapted from a dissertation
submitted to the University of Washington
in partial fulfillment of
the requirements for the degree of
Doctor of Philosophy

CONTENTS

NOTATION

$(\bar{\ })$	The horizontal mean (often just capitalized: $\bar{\tilde{\theta}} = T$, etc.)
$\langle\ \rangle$	The vertical mean over the mixed layer
$\tilde{b} = B + b$	Buoyancy
B^*	Parameter for relative importance of H^* to Ro^{-1} for cyclical steady state
$\overline{bw}$	Turbulent buoyancy flux
$\overline{cw}$	Complex turbulent momentum flux
c_p	Specific heat at constant pressure
C_D	Drag coefficient in quadratic wind stress law
$C = U + iV$	Mean horizontal velocity in complex form
$c = u + iv$	Turbulent horizontal velocity in complex form
d	Ekman depth of frictional resistance
d'	Surface production zone (Niiler); also used as a depth proportional to Ekman depth (d)
D	Total rate of viscous dissipation of turbulent kinetic energy in the mixed layer
D_s	Molecular diffusion coefficient
$\frac{1}{2}E = \frac{1}{2}u_i u_i = \frac{u^2 + v^2 + w^2}{2}$	Turbulent kinetic energy (per unit mass)
E^*	$\langle\bar{E}\rangle/(h\Delta B)$
$E^*_{11} + E^*_{22} + E^*_{33}$	Turbulent kinetic energy nondimensionalized with the friction velocity squared, u_*^2
$f = 2\lvert\vec{\Omega}\rvert\sin\phi$	Coriolis parameter

F	Damping force for inertial motions
g	Apparent gravitational acceleration
G	Total rate of mechanical production of turbulent kinetic energy in the mixed layer
h	Depth of mixed layer
h_r	Mixed layer depth if the vertical extent of the region is stationary or retreating
H^*	Mixed layer depth (h) non-dimensionalized with the Obukhov length
h_c	Compensation depth for radiative heating
J	Mechanical equivalent of heat, $4.186 \times 10^7 \frac{\text{gm cm}^2}{\text{cal sec}^2}$
K_0	Eddy mixing coefficient for neutral conditions
$K = K_m$	Eddy viscosity
K_T	Eddy conductivity
L	Obukhov length scale
ℓ	Integral turbulence length scale
ℓ_1	Convective length scale
ℓ_2	Rotational length scale
m_i , p_i	Model constants
n	Value for integrated flux Richardson number
N	Brunt-Väisälä frequency
p	Fluctuating pressure component
$\partial P_g / \partial x_\alpha$	Geostrophic pressure gradient in the ocean

$\overline{PE} + \overline{KE}$	Total mechanical energy per unit mass in the mixed layer
P^*	Nondimensional entrainment flux
Q	Radiation absorption
Q'	Solar heating function
Q_0	Solar radiation through interface (incident minus reflected)
$\frac{1}{2} q^2 = \frac{u^2 + v^2}{2}$	Horizontal component of turbulent kinetic energy
r	Fraction of net production going to potential energy by means of entrainment
Ro	Rossby number
Ri	Gradient Richardson number, $\frac{\partial B/\partial z}{\lvert \partial C/\partial z \rvert^2}$
RF	Flux Richardson number, $-\overline{bw} / \left(\overline{uw}\,\frac{\partial U}{\partial z} + \overline{vw}\,\frac{\partial V}{\partial z}\right)$
Ri_δ	Gradient Richardson number in the entrainment zone
Ri^*	Overall or bulk Richardson number, $h\Delta B/\lvert \Delta C \rvert^2$
Ri_T	Total Gradient Richardson number $= \frac{\partial \tilde{b}/\partial z}{(\partial \tilde{u}/\partial z)^2}$
$\tilde{s} = S + s$	Salinity
t	Time

$(\tilde{u}_i) = (U+u, V+v, W+w)$	Total instantaneous velocity, the sum of the mean and turbulent components (neglecting any geostrophic component)
U_g, V_g	Geostrophic components of velocity
u_e	dh/dt, entrainment velocity
u^*	Friction velocity, $\sqrt{\lvert\overline{cw}(0)\rvert}$
$u_* b_*$	Surface buoyancy flux, $-\overline{bw}(0)$
W	Wind velocity; sometimes used as mean vertical water velocity
W^*	Nondimensional entrainment velocity, $u_e/\sqrt{\langle\bar{E}\rangle}$
$(x_i) + (x,y,z)$	Rectangular space coordinates with $x_3 = z$ aligned vertically upward, parallel to the local apparent direction of gravity
α	$-\rho_0^{-1}\partial\rho/\partial S$
β	Coefficient of thermal expansion, $\rho_0^{-1}\partial\rho/\partial T$
$\gamma(z)$	Extinction coefficient for net solar radiation
Γ	$\partial B/\partial Z$ for $Z < (-h-\delta) = N^2$
Γ_T	$\partial T/\partial Z$ for $Z < (-h-\delta)$
δ'	Fraction of turbulent energy dissipated
δ	Thickness of entrainment zone
δC_0	Excess surface velocity, $C(z=0) - \langle C\rangle$
ΔB	Change in mean buoyancy, across the entrainment zone, $B(-h) - B(-h-\delta)$

$\lvert\Delta C\rvert$	Mean velocity drop across the density interface
ε	Rate of viscous dissipation of turbulent kinetic energy, $\nu\overline{\frac{\partial u_i}{\partial x_j}\frac{\partial u_i}{\partial x_j}}$
$\tilde{\eta} = \eta_0 e^{ik(x - c_1 t)}$	Internal wave amplitude on interface
$\tilde{\theta} = T + \theta$	Temperature
θ^*	Temperature flux scale, $b^*/\beta g$
κ	Thermal conductivity
Λ	Heaviside unit step function; also used as dissipation length scale
μ	Molecular viscosity
ν	Kinematic viscosity
$\tilde{\rho}$	The instantaneous density of the sea water
$\rho_0 = \rho(\theta_0, S_0)$	The density for representative values of salinity, s_0, and temperature, θ_0
ρ_a	Representative density of air
$\rho_0 C_p \overline{\theta w}$	Turbulent heat flux
$\lvert\vec{\tau}\rvert$	Surface stress, $\rho_0 u_*^2$
τ_ε	Dissipation time scale
τ^*	Dimensionless time scale, t/τ_ε
τ_I	Time constant for damping by F
ϕ	Latitude

ϕ^*	$E^*/Ri^* = \frac{\langle\bar{E}\rangle \lvert\Delta C\rvert^2}{(h\Delta B)^2}$
Ψ^*	Nondimensionalized turbulent kinetic energy, $h\langle\bar{E}\rangle / (u_*^3 \tau_\varepsilon)$
Ω_j	Earth's rotation vector
ω	Angular frequency

A GENERAL MODEL OF THE OCEAN MIXED LAYER USING A TWO-COMPONENT TURBULENT KINETIC ENERGY BUDGET WITH MEAN TURBULENT FIELD CLOSURE

Roland W. Garwood, Jr.

A non-stationary, one-dimensional bulk model of a mixed layer bounded by a free surface above and a stable nonturbulent region below is derived. The vertical and horizontal components of turbulent kinetic energy are determined implicitly, along with layer depth, mean momentum, and mean buoyancy. Both layer growth by entrainment and layer retreat in the event of a collapse of the vertical motions due to buoyant damping and dissipation are predicted. Specific features of the turbulent energy budget include mean turbulent field modeling of the dissipation term, the energy redistribution terms, and the term for the convergence of buoyancy flux at the stable interface (making possible entrainment). An entrainment hypothesis dependent upon the relative distribution of turbulent energy between horizontal and vertical components permits a more general application of the model and presents a plausible mechanism for layer retreat with increasing stability. A limiting dissipation time scale in conjunction with this entrainment equation results in a realistic cyclical steady-state for annual evolution of the upper-ocean density field. Several hypothetical examples are solved, and a real case is approximated to demonstrate this response. Of particular significance is the modulation of longer-period trends by the diurnal-period heating/cooling cycle.

1. INTRODUCTION

1.1 Purpose of the Study

The objective of this study is the formulation of a unified mathematical model of the one-dimensional, nonstationary oceanic turbulent boundary layer. In particular, this model should help explain and predict the development in time of the seasonal pycnocline.

Interest in the ocean mixed layer stems from both theoretical and practical considerations. Thermal energy and mechanical energy received from the atmosphere not only control the local dynamics, but the layer itself modulates the flux of this energy to the deeper water masses. Conversely, flux of heat back to the atmospheric boundary layer has an important influence upon the climate and its fluctuations. Figure 1 depicts the mechanical energy budget for the ocean mixed layer.

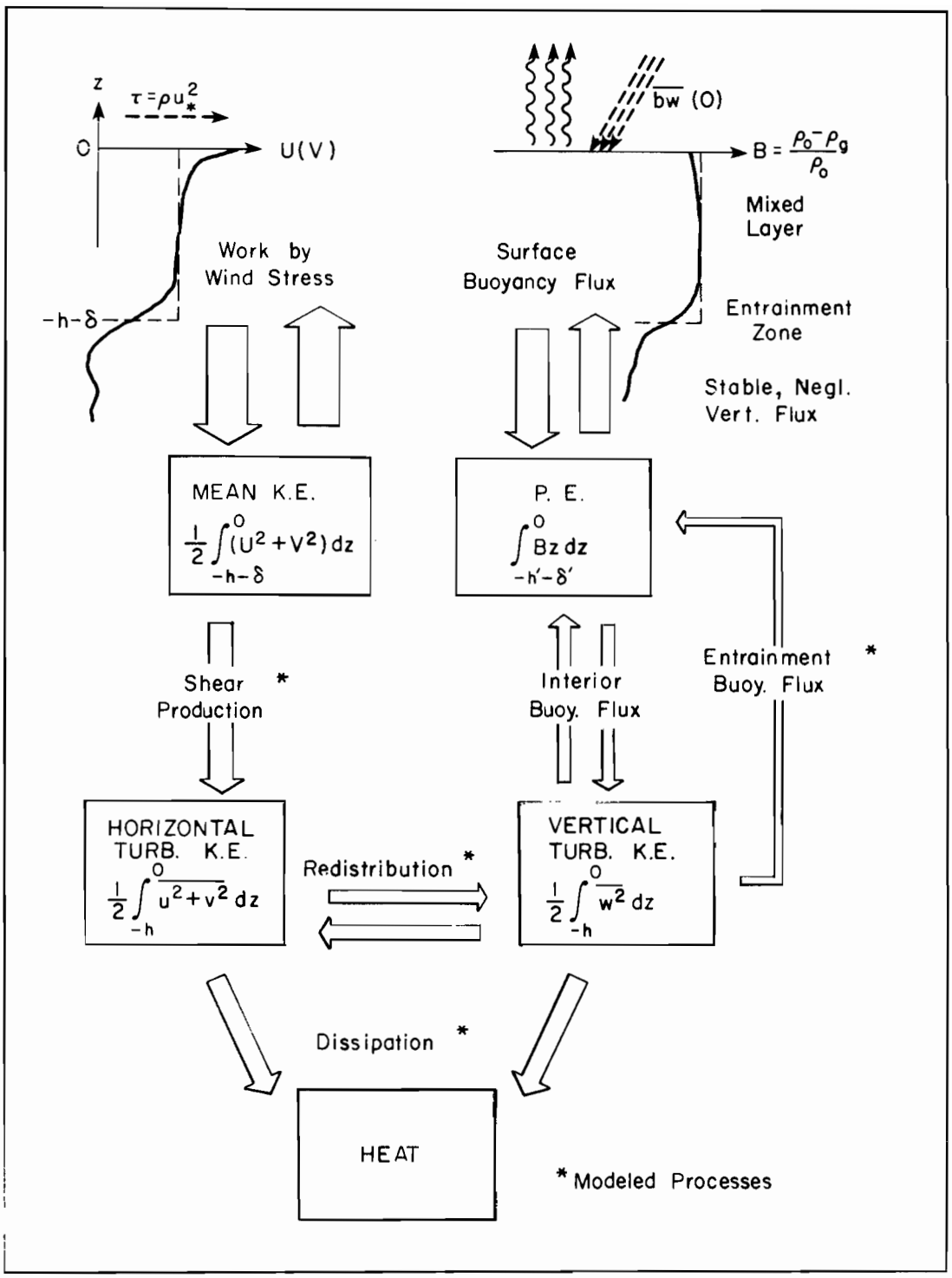

Figure 1. Mechanical energy budget for the ocean mixed layer.

In addition to climatological and ocean circulation studies, other applications of a practical model of the mixed layer include investigations of advection and turbulent dilution of dissolved or suspended concentrations of matter such as pollutants and nutrients. Prediction of entrainment of the deeper, nutrient-rich water into the mixed layer has particular pertinence to the estimation of primary productivity.

The need to further develop and attempt to improve the one-dimensional mixed-layer model is evident. The failure of earlier models to consistently explain the annual cycle of thermocline development is, for the most part, not attributable to the assumption of one-dimensionality.

A refined treatment of the often neglected terms of the turbulent kinetic energy budget promises to improve the physical understanding of the turbulent ocean boundary layer and make possible the creation of a better-performing model.

A detailed review of the literature associated with mixed-layer modeling is undertaken in Chapter II, but Table 1 summarizes the major historical contributions to the understanding of the physics of the mixed layer.

The works of primary concern here are those dealing explicitly with equations for the production, alteration, and destruction of turbulent kinetic energy within the mixed layer. Kraus and Turner (1967) were the first to heed the turbulent kinetic energy budget in a one-dimensional mixed layer model, utilizing the approximately decoupled state of the equations for the thermal and mechanical energies. By neglect of the frictional generation of heat, the vertically integrated heat equation becomes a relationship for the conservation of potential energy. However, viscous dissipation cannot be neglected in the turbulent energy budget, and Geisler and Kraus (1969) as well as Miropol'skiy (1970) and Denman (1973) added it to the basic model. Niiler (1975) showed that in addition to the equations for thermal (potential) and turbulent (kinetic) energy, an equation for the mean kinetic energy should properly be incorporated because entrainment converts some of the mean flow energy into turbulent energy, over and above the parameterized wind-stress production.

Further questions remain and limit the general applications of these earlier models:

a. The viscous dissipation of turbulent energy has been parameterized as a fixed fraction of the wind-stress production and hence is a function of the surface friction velocity u_*. Dissipation may be related to the integral velocity scale of the turbulence, but this scale is not always proportional to u_*. Surface heat (buoyancy) flux and entrainment fluxes can contribute significantly to the turbulent intensity.

b. Entrainment may also be considered a function of the ambient turbulence parameters. Instabilities leading to entrainment are probably induced by horizontal turbulent velocities locally at the bottom of the mixed layer, so the entrainment rate doesn't necessarily correspond to an integral constraint upon the total turbulent energy budget.

Table 1. Summary of Historical Contributions

Date	Author(s)	Contribution
1905	Ekman	Constant eddy viscosity solution to steady-state momentum equation: Ekman spiral; "depth of frictional influence"; suggested $h \propto W/\sqrt{\sin \phi}$.
1935	Rossby and Montgomery	Improved current measurements to demonstrate $h \simeq u_*/f$ (Rossby number $\simeq$ constant).
1948	Munk and Anderson	Simultaneous solution of steady-state heat and momentum equations using eddy mixing coefficients variable with Richardson number.
1960	Kitaigorodsky	Using dimensional analysis, suggested that $h \simeq L$, the Obukhov length scale.
1961	Kraus and Rooth	Penetration of solar radiation to depth makes steady-state possible for heat equation because of surface heat loss by conduction, evaporation, and long wave radiation; unstable density profile above compensation depth (h_c) is source of turbulent kinetic energy produced by convection.
1967	Kraus and Turner	Included mechanical stirring (parameterized in terms of wind stress) as well as convective production as important source of turbulence for mixing: turbulent kinetic energy equation and heat equation form two-equation model in two unknowns--T, h; non-steady-state solutions and "retreating" (h) possible; viscous dissipation neglected.
1969	Geisler and Kraus	First "slab" model in which momentum equation is solved together with turbulent energy equation and heat equation; layer assumed homogeneous in T and U, V and hence moves as a slab; assumed buoyancy flux is fixed portion of mechanical production--essentially same as Kraus and Turner; applied model to atmosphere with subsidence.
1970	Miropol'skiy; Denman	Assumed dissipation a fixed fraction of mechanical production; remaining turbulent kinetic energy goes to buoyancy flux downwards including entrainment; essentially same as Kraus and Turner.
1973	Pollard, Rhines and Thompson	Slab model applied to ocean mixed layers; used total mechanical energy equation (rather than turbulent equation) plus momentum and heat equations; h, T, U, V--all functions of time. Ignored effects of turbulent energy budget altogether.
1974	Niiler	Re-emphasized the need to use the turbulent kinetic energy budget apart from the total mechanical energy budget; divided region into three sub-regions with no mechanical production in most of the mixed layer. Included turbulent kinetic energy produced by entrainment of zero-velocity water into moving slab, but surface mechanical production minus dissipation still parameterized in terms of u_*. Dissipation is not affected by the additional entrainment production, possibly causing a too-large entrainment rate.

c. The use of the total turbulent energy equation and consequently the neglect of energy redistribution among components also results in a somewhat inconsistent method of predicting layer "retreat." The consideration of separate budgets for the horizontal and vertical turbulent energy components will permit a more consistent interpretation of both entraining and retreating mixed layers.

In this paper, ad hoc mean turbulent field modeling of the terms in the turbulent kinetic energy equations permits the inclusion of these often salient effects in a generalized one-dimensional model of the ocean mixed layer.

2. CHARACTERISTICS OF THE OCEAN MIXED LAYER

The ocean mixed layer is defined as that fully-turbulent region of the upper ocean bounded on top by the sea-air interface. The wind and intermittent upward buoyancy flux attributable to surface cooling are the primary sources of mechanical energy for the mixing.

The most distinctive feature of this layer and what really defines its extent is its relatively high intensity of continuous, three-dimensional turbulent motion. Vertical turbulent fluxes within the mixed layer can be so much greater than vertical fluxes in the underlying stable water column that the dynamics of the layer are essentially decoupled from the underlying region. (Of course the dynamics of the underlying water masses are probably very dependent upon the mixed layer.)

Typically, an actively entraining mixed layer is bounded on the bottom by a sharp density discontinuity separating the layer from a stable, essentially nonturbulent thermocline. Minimal stress at the bottom together with high turbulence intensity results in an approximate vertical uniformity in mean velocity and density. This ostensible homogeneity is the root of the term "slab," often used to describe the layer. On the other hand, only small gradients in these mean variables give rise to large turbulent fluxes. Therefore, even the slight non-homogeneity is highly important in the physics of the region and should not be neglected at the outset.

The nearly zero-flux state of the underlying thermocline causes the bottom boundary condition of the mixed layer to act almost as a slip condition on the mean velocity. This in turn creates a trap for inertial motion.

Deepening of the mixed layer is accomplished by entrainment of the more-dense underlying water into the turbulent region above. This process entails a potential energy increase and cannot take place without an energy source--the turbulent kinetic energy of the mixed layer above.

A simplified picture of the region is shown in Figure 2. There is an appealing practical aspect to the judicious use of the assumption of vertical homogeneity. This assumption permits the use of the vertically integrated

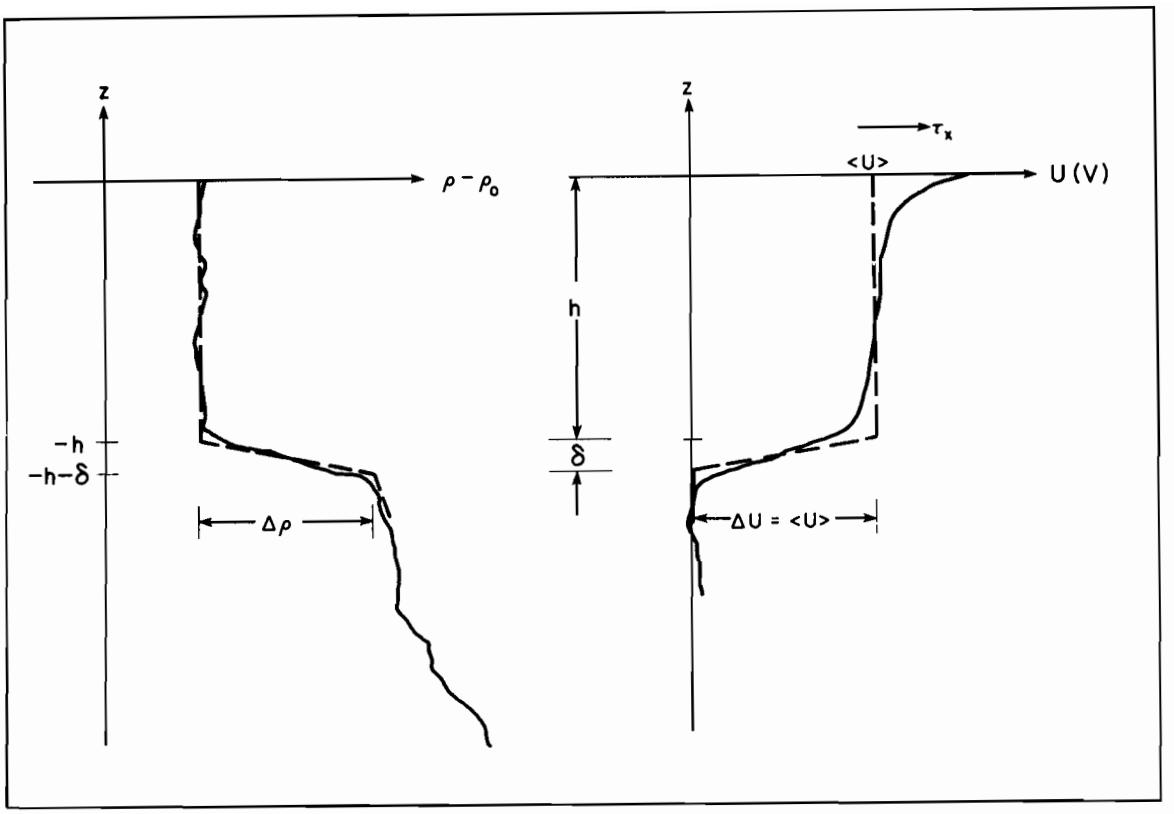

Figure 2. Idealized model for ocean mixed layer (----). Mixed layer depth is (h); (δ) is the thickness of the interface or entrainment zone.

momentum and heat (buoyancy) equations, thus avoiding the turbulent flux (of momentum and buoyancy) closure problem altogether.

The depth of the oceanic wind-mixed surface layer is typically on the order of ten to a hundred meters. The horizontal scale size is that of the radius of the circle of inertia--seldom larger than a few kilometers in temperate latitudes. These two dominant scale sizes are usually significantly smaller than the horizontal scale sizes of the driving meteorological disturbances, water mass features, and distance to lateral boundaries. Therefore, the approximation of local horizontal homogeneity for all mean variables is usually accurate and is a basic assumption of this work. The local consequence of some lateral inhomogeneity can be parameterized without qualitatively undermining such a one-dimensional model. For example, a divergence of the horizontal current field results in a nonzero vertical mean velocity which in itself can be assumed locally uniform in the horizontal. A minor rate of loss (compared with the surface flux) of mean momentum by lateral and/or downward radiation of inertial motion may be parameterized also without compromising the dominant processes.

Substantial barotropic and baroclinic features in the mean fields can be linearly superimposed. The mean fields of concern are therefore the horizontally homogeneous components of the total fields. In particular, the

momentum equation has the geostrophic component subtracted out, eliminating any lateral pressure gradient.

1.3 Fundamental Principles and Equations

The underlying principles employed in studying the mixed layer are the combined conservations of mass, momentum, thermal energy, and mechanical energy.

The conservation of momentum and the condition of incompressibility are reflected by the Navier-Stokes equations of motion, invoking the Boussinesq approximation:

$$\rho_0 \frac{\partial \tilde{u}_i}{\partial t} + \rho_0 \tilde{u}_j \frac{\partial \tilde{u}_i}{\partial x_j} + \rho_0 \varepsilon_{ijk} \Omega_j \tilde{u}_k + \frac{\partial \tilde{p}}{\partial x_i} - (\rho_0 - \tilde{\rho}) g \delta_{i3} = \mu \frac{\partial^2 \tilde{u}_i}{\partial x_j \partial x_j} \quad . \tag{1.1}$$

$$\frac{\partial \tilde{u}_i}{\partial x_i} = 0 \quad . \tag{1.2}$$

Because frictional generation of heat is negligible compared with typical magnitudes for the divergence of heat flux, the conservation of thermal energy is decoupled from the mechanical energy budget, and the first law of thermodynamics for an incompressible fluid gives the heat equation.

$$\frac{\partial \tilde{\theta}}{\partial t} + \tilde{u}_j \frac{\partial \tilde{\theta}}{\partial x_j} = \frac{\kappa}{\rho_0 C_p} \frac{\partial^2 \tilde{\theta}}{\partial x_j \partial x_j} + \frac{Q}{\rho_0 C_p} \quad . \tag{1.3}$$

The conservation of salt mass is of the same form, but it lacks a term analogous to the radiation absorption term, Q.

$$\frac{\partial \tilde{s}}{\partial t} + \tilde{u}_j \frac{\partial \tilde{s}}{\partial x_j} = D_s \frac{\partial^2 \tilde{s}}{\partial x_j \partial x_j} \quad . \tag{1.4}$$

A simplified but sufficiently accurate equation of state for local and reasonably short-term application in the mixed layer is given by

$$\tilde{\rho} = \rho_0 [1 - \beta(\tilde{\theta} - \theta_0) + \alpha(\tilde{s} - s_0)] \tag{1.5}$$

where $\rho_0 = \tilde{\rho}(\theta_0, s_0)$ is a representative but arbitrary density at the time and location of consideration. The coefficients (β) and (α) are assumed to remain constant.

Taking the scalar product of $(\tilde{u}_i)$ with the respective terms of equation (1.1), the mechanical energy equation is formed,

$$\frac{\partial}{\partial t}\left(\frac{\tilde{u}_i\tilde{u}_i}{2}\right) + \tilde{u}_j \frac{\partial}{\partial x_j}\left(\frac{\tilde{u}_i\tilde{u}_i}{2}\right) + \frac{\tilde{u}_i}{\rho_0}\frac{\partial \tilde{p}}{\partial x_i} - \tilde{b}\tilde{u}_3 = \nu \tilde{u}_i \frac{\partial^2 \tilde{u}_i}{\partial x_j \partial x_j} , \qquad (1.6)$$

where the buoyancy ($\tilde{b}$) is given by

$$\tilde{b} = \left(\frac{\rho_0 - \tilde{\rho}}{\rho_0}\right) g \quad . \qquad (1.7)$$

Assuming horizontal homogeneity of mean variables, where the horizontal mean is defined by

$$\overline{(\tilde{f})}\,(z,t) = \lim_{X\to\infty} \frac{1}{X^2} \int_{\frac{-X}{2}}^{\frac{X}{2}} \int_{\frac{-X}{2}}^{\frac{X}{2}} \tilde{f}(x,y,z,t)\, dxdy \quad ,$$

and separating all variables into mean and fluctuating components gives

$$\left\{\tilde{u}_i\right\} = \begin{Bmatrix} U_g + U(z,t) + u(x,y,z,t) \\ V_g + V(z,t) + v(x,y,z,t) \\ 0 + w(x,y,z,t) \end{Bmatrix} \quad .$$

$$\theta = T(z,t) + \theta(x,y,z,t) \quad .$$

$$\tilde{p} = Pg + p(x,y,z,t) \quad .$$

$$\tilde{b} = B(z,t) + b(x,y,z,t) \quad .$$

Strictly speaking, the total fluctuating part of each variable includes a component directly attributable to surface and internal wave motion. This

component has been removed from the fields depicted above. The virtually irrotational wave velocities are assumed noninteractive except as an external source or sink of turbulent energy due to the net contributions of breaking surface waves and radiating internal waves.

In practice, a time mean is employed in data analysis rather than even the horizontal mean. Ideally, the averaging time should be short compared with the time necessary for significant changes in the mean fields but long compared with the integral time scale of the turbulence.

$$B(z,t) = \overline{(\tilde{b})} \simeq \frac{1}{\Delta t} \int_{-\frac{\Delta t}{2}}^{+\frac{\Delta t}{2}} \tilde{b}\, dt, \text{ for example.}$$

In making the Boussinesq approximation, the hydrostatic component of pressure has already been eliminated. The remaining mean pressure is assumed to be geostrophic:

$$\frac{\partial P_g}{\partial x} = \rho_0 f V_g . \tag{1.8a}$$

$$\frac{\partial P_g}{\partial y} = - \rho_0 f U_g . \tag{1.8b}$$

Subtracting the geostrophic equations from the total momentum equation and dropping the negligible viscous terms, the equations for the mean momentum become in complex notation (for the sake of brevity)

$$\frac{\partial C}{\partial t} = - ifC - \frac{\partial \overline{cw}}{\partial z} , \tag{1.9}$$

where $C = U + i V$ and $c = u + i v$.

Using equations (1.3), (1.4), (1.5), and (1.7) and again neglecting molecular fluxes, a buoyancy equation is formed:

$$\frac{\partial \tilde{b}}{\partial t} + \tilde{u}_j \frac{\partial \tilde{b}}{\partial x_j} = \frac{\beta g}{\rho_0 C_p} Q . \tag{1.10}$$

Equation (1.11) is the mean buoyancy equation.

$$\frac{\partial B}{\partial t} = - \frac{\partial \overline{bw}}{\partial z} + \frac{\beta g}{\rho_0 C_p} Q \ . \tag{1.11}$$

The use of a buoyancy equation reflecting the combined conservations of thermal energy and dissolved material is not only more general than a heat equation alone, but it makes more obvious the coupling with the mechanical energy budget.

Using the decomposition into mean and fluctuating parts and taking the mean of equation (1.6) yields the mean equation for the total mechanical energy. Where $E = u_i u_i = u^2 + v^2 + w^2$,

$$\frac{\partial}{\partial t}\left(\frac{U^2 + V^2}{2} + \frac{\overline{E}}{2}\right) + \frac{\partial}{\partial z}\left[\overline{w\left(\frac{E}{2} + \frac{p}{\rho_0}\right)}\right] + \frac{\partial}{\partial z}\left[U\,\overline{uw} + V\,\overline{vw}\right] = \left[\overline{bw}\right] - \left[\nu\,\overline{\frac{\partial u_i}{\partial x_j}\,\frac{\partial u_i}{\partial x_j}}\right] . \tag{1.12}$$

The viscous diffusion and viscous dissipation of the mean kinetic energy are negligible and have been dropped in equation (1.12).

The turbulent kinetic energy equation is formed by subtracting the scalar produce of (U_i) and equation (1.9) from equation (1.12).

$$\frac{1}{2}\frac{\partial \overline{E}}{\partial t} + \frac{\partial}{\partial z}\left[\overline{w\left(\frac{p}{\rho_0} + \frac{E}{2}\right)}\right] + \left[\overline{uw}\,\frac{\partial U}{\partial z} + \overline{vw}\,\frac{\partial V}{\partial z}\right] = \left[\overline{bw}\right] - \left[\varepsilon\right] . \tag{1.13}$$

The budgets for the individual components of turbulent energy are formed in the same manner from equation (1.1) by setting i = 1,2,3 without summation:

$$\frac{1}{2}\overline{\frac{\partial u^2}{\partial t}} = - \overline{uw}\,\frac{\partial U}{\partial z} - \frac{\partial}{\partial z}\left(\overline{\frac{wu^2}{2}}\right) + \overline{\frac{P}{\rho_0}\,\frac{\partial u}{\partial x}} + \Omega_3\,\overline{uv} - \Omega_2\,\overline{uw} - \frac{\varepsilon}{3} \ . \tag{1.14a}$$

$$\frac{1}{2}\overline{\frac{\partial v^2}{\partial t}} = - \overline{vw}\,\frac{\partial V}{\partial z} - \frac{\partial}{\partial z}\left(\overline{\frac{wv^2}{2}}\right) + \overline{\frac{P}{\rho_0}\,\frac{\partial v}{\partial y}} - \Omega_3\,\overline{uv} - \frac{\varepsilon}{3} \ . \tag{1.14b}$$

$$\frac{1}{2}\ \overline{\frac{\partial w^2}{\partial t}} = \overline{bw} - \frac{\partial}{\partial z}\left(\overline{\frac{w^3}{2}} + \overline{\frac{wp}{\rho_0}}\right) + \overline{\frac{P}{\rho_0}\frac{\partial w}{\partial z}} + \Omega_2\ \overline{uw} - \frac{\varepsilon}{3}\ . \qquad (1.14c)$$

Notice that the orientation of the horizontal axes is (x) positive to the east and (y) positive to the north. The rate of viscous dissipation $\varepsilon = \nu\ \overline{\partial u_i \partial u_i / \partial x_j \partial x_j}$ behaves like $(\bar{E}/\tau_\varepsilon)$ and the small size of the dissipation time constant ($\tau_\varepsilon \sim h/\sqrt{\bar{E}}$) compared with the time scale of the meteorological forcing causes the intensity of the turbulence to track along in a quasi-steady state with a continually changing net rate of production. Hence the time rate of change of turbulent kinetic energy is usually much smaller than the other terms of (1.13) and thus may be neglected. Because viscous dissipation of energy occurs primarily in the range of wave numbers that exhibit local isotropy (the equilibrium range), dissipation (ε) is divided equally among the component budgets (1.14 a-c).

The second term in equation (1.13) is the divergence of the turbulent flux of kinetic energy. Over the whole mixed layer, it probably accounts for a net gain of energy. Wind-wave interactions at the surface result in some net downward flux, primarily from breaking surface waves. If the Brunt-Väisälä frequency (N) of the adjacent underlying stable water column is sufficiently large so as to be comparable with the frequency of the integral scale of the turbulence, turbulent energy may be lost to the generation of internal waves. One of the most significant aspects of this term is that locally, at the bottom of the layer during occasions of entrainment, a net convergence of flux of energy is necessary to maintain the downward buoyancy flux for a deepening mixed layer.

The third term, the rate of mechanical production, is perhaps the dominant source of turbulent kinetic energy. It is the rate of conversion of mean to turbulent kinetic energy by the turbulent flux of momentum downgradient.

The last term on the left, the buoyancy flux, locally within the mixed layer can be either a sink or a source. Usually, however, the mixed region is slightly stable overall, and this term represents the rate of increase of potential energy by fluxing buoyancy downward. During instances of large buoyancy flux up across the surface, this term can become an important source as in the case of strong convective cooling in the autumn.

The summation of separate component equations yields (1.13), but one term that is very important in mixed layer dynamics sums to zero and therefore appears only in the component budgets (1.14 a-c). This term is the correlation between pressure and rate of strain, $p/\rho_0\ \partial u_\alpha/\partial x_\alpha$. Since it sums to zero by continuity, it causes only a redistribution of energy among $\overline{u^2}$, $\overline{v^2}$, and $\overline{w^2}$.

The individual turbulent energy budgets also have redistribution terms due to rotation of the Earth, but these shall be neglected because of the usually short integral time scale in comparison with one day. Perhaps this

effect does become significant in some of the very deep convective mixed layers that are not limited in growth by a permanent pycnocline.

Application of the vertical homogeneity assumption to the momentum and buoyancy equations (1.9) and (1.11) gives relationships for the turbulent fluxes in terms of the boundary conditions (specified externally) alone:

$$\overline{cw}\,(z) = \overline{cw}\,(0)\,\left(1 + \frac{z}{h}\right) + \Delta C\,\left(\frac{z}{h}\right)\frac{dh}{dt}\,; \tag{1.15}$$

$$\overline{bw}\,(z) = \overline{bw}\,(0)\,\left(1 + \frac{z}{h}\right) + \frac{z}{h}\left[\Delta B\,\frac{dh}{dt} - \frac{\beta g}{\rho_0 C_p}\int_{-h}^{0} Q\,dz\right] - \frac{\beta g}{\rho_0 C_p}\int_{z}^{0} Q\,dz\,. \tag{1.16}$$

The integral of (1.16) over the mixed layer gives the net buoyant damping for the whole layer.

$$-\int_{-h-\delta}^{0} \overline{bw}\,dz = \frac{h}{2}\left[\Delta B\,\frac{dh}{dt} - \overline{bw}\,(0)\right] - \frac{\beta g}{\rho_0 C_p}\int_{-h-\delta}^{0}\left[\frac{Qh}{2} - \int_{z}^{0} Q\,d\lambda\right] dz\,. \tag{1.17}$$

Integrating the turbulent kinetic energy equations from $z = (-h-\delta)$ to $z = 0$ gives

$$\frac{1}{2}\frac{d}{dt}\left(\langle\overline{E}\rangle h\right) = \int_{-h-\delta}^{0}\left(-\overline{uw}\,\frac{\partial U}{\partial z} - \overline{vw}\,\frac{\partial V}{\partial z} + \overline{bw} - \varepsilon\right) dz - \left[\overline{w\left(\frac{E}{2} + \frac{p}{\rho_0}\right)} + \frac{\overline{wp}}{\rho_0}\right]_{-h-\delta}^{0}. \tag{1.18}$$

$$\frac{1}{2}\frac{d}{dt}\left(\overline{\langle u^2\rangle h}\right) = \int_{-h-\delta}^{0}\left(-\overline{uw}\,\frac{\partial U}{\partial z} + \overline{\frac{p}{\rho_0}\frac{\partial u}{\partial x}}\right) dz - \left[\frac{\overline{wu^2}}{2}\right]_{-h-\delta}^{0} - \frac{1}{3}\int_{-h-\delta}^{0} \varepsilon\,dz\,. \tag{1.19a}$$

$$\frac{1}{2}\frac{d}{dt}\overline{(\langle v^2\rangle h)} = \int_{-h-\delta}^{0}\left(-\overline{vw}\frac{\partial V}{\partial z} + \overline{\frac{p}{\rho_0}\frac{\partial v}{\partial y}}\right)dz - \left.\overline{\frac{wv^2}{2}}\right]_0 - \frac{1}{3}\int_{-h-\delta}^{0}\varepsilon\,dz \ . \tag{1.19b}$$

$$\frac{1}{2}\frac{d}{dt}\overline{(\langle w^2\rangle h)} = \int_{-h-\delta}^{0}\left(\overline{bw} + \overline{\frac{p}{\rho_0}\frac{\partial w}{\partial z}}\right)dz - \left.\overline{w\left(\frac{w^2}{2} + \frac{p}{\rho_0}\right)}\right]_0 + \left.\overline{\frac{wp}{\rho_0}}\right]_{-h-\delta} - \frac{1}{3}\int_{-h-\delta}^{0}\varepsilon\,dz \ . \tag{1.19c}$$

The surface boundary conditions are prescribed functions of time:

$$-\overline{uw}\,(0) = \frac{\tau_x(t)}{\rho_0} \ . \tag{1.20a}$$

$$= \overline{vw}\,(0) = \frac{\tau_y(t)}{\rho_0} \ . \tag{1.20b}$$

$$-\overline{bw}\,(0) = g\,[\alpha\,\overline{sw}\,(0,t) - \beta\,\overline{\theta w}\,(0,t)] \ . \tag{1.21}$$

Also to be prescribed in deriving the system is the radiation absorption function, $Q\,(z,t)$.

The boundary conditions at the bottom of the mixed layer, $z = -h$, will, on the other hand, conform to the developing situation. To derive these conditions, the equations (1.9) and (1.11) are integrated over the entrainment zone from $z = (-h-\delta)$ to $z = (-h)$:

$$\delta/h \overset{\lim}{\to} 0 \int_{-h-\delta}^{-h}\frac{\partial U}{\partial t}\,dz = [U\,(-h) - U\,(-h-\delta)]\ \frac{dh}{dt} = \Delta U\,\frac{dh}{dt} \ .$$

$$\lim_{\delta/h \to 0} \int_{-h-\delta}^{-h} f\, V\, dz = 0 \ .$$

$$\int_{-h-\delta}^{-h} - \frac{\partial \overline{uw}}{\partial z}\, dz = - \overline{uw}\,(-h) \ .$$

Therefore

$$- \overline{uw}\,(-h) = \Delta U \frac{dh}{dt} \ , \qquad \text{and similarly}$$

$$- \overline{vw}\,(-h) = \Delta V \frac{dh}{dt} \ , \qquad \text{or in complex}$$

notation,

$$- \overline{cw}\,(-h) = \Delta C \frac{dh}{dt} \ . \tag{1.22}$$

Also,

$$- \overline{bw}\,(-h) = \Delta B \frac{dh}{dt} \tag{1.23}$$

where $\Delta C = \Delta U + i\Delta V$ and ΔB are the respective jumps in the values of the mean variables across the density interface separating the mixed layer from the nonturbulent region below. The discontinuity need not be a perfect one ($\delta = 0$) for the boundary conditions (1.22) and (1.23) to be valid. A sufficient condition is for the fluxes of momentum and buoyancy from the mixed layer into the interface zone, resulting in a lowering of the vertical position of the zone, to be much larger than that portion of the fluxes contributing to changes in the momentum and buoyancy profiles of the moving interface zone itself.

Integrating equations (1.9) and (1.11) from ($z = -h - \delta$) to ($z = 0$) provides a form of the equations that includes the effects of the entrainment stress and entrainment buoyancy flux of (1.22) and (1.23).

$$h \frac{d\langle C\rangle}{dt} + \Delta C \frac{dh}{dt} \Lambda = - if\langle C\rangle h - \overline{cw}\,(0) \tag{1.24}$$

and

$$h \frac{d\langle B \rangle}{dt} + \Delta B \frac{dh}{dt} \Lambda = \frac{\beta g}{\rho_0 C_p} \int_{-h-\delta}^{0} Q \, dz - \overline{bw}\,(0) \qquad (1.25)$$

where the Heaviside unit step function, Λ, is dependent upon (dh/dt).

$$\Lambda \left(\frac{dh}{dt}\right) = \begin{cases} 1 \text{ for } \frac{dh}{dt} > 0 \\ 0 \text{ for } \frac{dh}{dt} \leq 0 \end{cases} \qquad (1.26)$$

and < > denotes a vertical mean for the mixed layer:

$$\langle C \rangle = \frac{1}{h+\delta} \int_{-h-\delta}^{0} C \, dz, \text{ etc.}$$

1.4 Course of Action in Attacking the Problem

To lay a foundation and present a perspective of the problem at hand, the literature treating models of the surface mixed layer is reviewed relative to the basic principles and general equations laid down in the previous sections. This approach organizes the historical work in terms of the fundamentals, and it provides the stepping stones for the development of this research.

The turbulent kinetic energy budget is examined closely. The role of the previously neglected redistribution terms is assessed. All of the terms are modeled by use of mean-turbulent-field techniques, permitting the eventual implicit solution for the turbulent energy content of the mixed layer.

The final preparatory work needed to complete the model is treated in a chapter on entrainment. This includes the derivation of an equation relating the rate of entrainment (dh/dt) to the other variables.

The final numerical method of solution of the nonstationary, non-linear set of equations permits the solution of hypothetical cases as well as the simulation of field observations. The numerical model requires as input the initial conditions of density and current and the surface boundary flux of buoyancy (heat and/or salinity) and surface wind stress as functions of time. Model outputs include the mean density profile, the turbulent kinetic energy, and the mixed-layer depth, all as functions of time.

2. REVIEW OF THE LITERATURE

2.1 Ekman Depth of Frictional Resistance

V. Walfrid Ekman (1905) originated the concept of a "depth of frictional resistance" for the upper section of a wind-stressed ocean. This depth (d) comes from the mathematical solution to the steady state horizontal momentum equation, (1.9), in which the Reynolds stress is related to the mean shear by a constant eddy viscosity (K).

$$\frac{\partial C}{\partial t} = - ifC - \frac{\partial \overline{cw}}{\partial z} \tag{1.9}$$

where $$\frac{\partial C}{\partial t} = 0$$

and $$- \overline{cw} = K \frac{\partial C}{\partial z} .$$

Then $$0 = - ifC + K \frac{d^2C}{dz^2} . \tag{2.1}$$

If the boundary conditions are

$$- \overline{cw} (0) = u_*^2 + i\, 0$$

and

$$- \overline{cw} (-\infty) = 0 ,$$

the solution is

$$C(z) = \frac{u_*^2}{\sqrt{Kf}} \left[\sin \left(\frac{\pi z}{d} + \frac{\pi}{4} \right) - i \cos \left(\frac{\pi z}{d} + \frac{\pi}{4} \right) \right] e^{\frac{\pi z}{d}} \tag{2.2}$$

where $$d = \pi \sqrt{\frac{2K}{f}} \quad . \tag{2.3}$$

At the depth ($z = - d$) the direction of the flow is opposite to the surface current and the magnitude has been reduced to ($e^{-\pi}$) times the surface magnitude.

Classical thought has suggested that any surface layer mixed by the action of the wind should have a depth that is of the same order as (d).

Using a quadratic law relating windspeed (W) to surface stress

$$\rho_0 u_*^2 = C_D \rho_a W^2 \tag{2.4}$$

and an empirical relation from observations,

$$|C(0)| = \frac{0.0127\ W}{\sqrt{\sin \phi}}\ , \tag{2.5}$$

Ekman derived a formula for (d) as a function of wind speed and latitude (ϕ):

$$d = 7.5\ \sec^{-1} \frac{W}{\sqrt{\sin \phi}}\ . \tag{2.6}$$

2.2. Rossby Number

Rossby and Montgomery (1935) pointed out that the depth (h) of a surface drift current layer and Ekman's depth of frictional resistance (d) are not necessarily comparable: the depth (h) has a definite physical meaning, but (d) designates only the theoretical rate of exponential decay for a system obeying (2.1).

Rossby and Montgomery derived the formula ($h \propto W/\sin \phi$) or, equivalently

$$h \propto u_*/f \tag{2.7}$$

where the constant of proportionality is the Rossby number, $R_0 = u_*/hf$. They then presented measurements demonstrating the greater validity of (2.7) in comparison with (2.6.)

It should be recognized, however, that Ekman's result differs from that of Rossby and Montgomery only because of the use of the relation (2.5.) If instead of applying this empirical constraint, the eddy viscosity (K) is modeled in terms of likely turbulent length and velocity scales ($K \sim u_* h$) and is assumed to be constant with depth, then ($d = 2\pi^2 u_*/f$) and the quadratic stress law gives

$$d \propto \frac{W}{(\sin \phi)\Omega}\ . \tag{2.8}$$

So, in spite of suggesting a distinction between the mixed layer depth and the depth of frictional resistance, Rossby and Montgomery obtained a result perhaps more comparable with that of Ekman than with the real situation. This was the case because both derivations considered only the momentum budget, neglecting the effects of buoyancy and mechanical energy upon the vertical fluxes of buoyancy and momentum within this turbulent oceanic boundary layer.

2.3 Eddy Transfer Coefficients in a Steady-State Problem

Munk and Anderson (1948) first combined the two problems of density structure and current structure into a unified theory on a steady-state thermocline. Like Ekman, they proposed an eddy viscosity (K_m) plus an eddy conductivity (K_h), but these parameters were made variable with the local gradient Richardson number (Ri).

$$Ri = \frac{(\partial B/\partial z)}{(\partial U/\partial z)^2} . \tag{2.9}$$

This model therefore included some of the effects of the turbulent energy budget.

$$K_{m,H} = \frac{KO}{(1 + C_{m,H}\, Ri)}\, n_{m,H} . \tag{2.10}$$

This function for the eddy viscosity and eddy conductivity was chosen because of its asymptotic behavior for small and large values of (Ri):

$$\lim_{Ri \to 0} K_{m,H} = KO, \text{ coefficient for no density gradient}$$

$$\lim_{Ri \to \infty} K_{m,H} = 0, \text{ for extreme stability.}$$

Because Munk and Anderson assumed steady state and did not recognize the presence of a sharp interface marking a boundary between the fully-turbulent mixed layer and the essentially quiescent stable region below, their results still resembled Ekman's original solution more than they do the physical reality.

2.4 Obukhov Length Scale

The more recent efforts in modeling the oceanic mixed layer started with a one-dimensional steady-state study by Kitaigorodsky (1960). Assuming that the ocean surface mixed layer was analogous to the constant-flux atmospheric

surface layer (as in Businger et al., 1971), Kitaigorodsky concluded by dimensional analysis that the mixed layer depth must be proportional to the Obukhov length, L.

For Kitaigorodsky's assumptions, the momentum and buoyancy equations, (1.9) and (1.11), reduce to

$$\frac{\partial \overline{cw}}{\partial z} = 0 \tag{2.11}$$

and

$$\frac{\partial \overline{bw}}{\partial z} = 0 \ . \tag{2.12}$$

The radiation absorption, Q, was assumed to be confined to the immediate surface layers. Taking the x-direction to be in the direction of the wind, the solutions to equations (2.11) and (2.12) are

$$-\overline{cw} = \text{constant} \equiv u_*^2$$

and

$$-\overline{bw} = \text{constant} \equiv u_* b_*$$

where (u_*^2) and $(u_* b_*)$ are the downward surface fluxes of momentum and buoyancy.

If the depth of the surface mixed layer (h) is dependent only upon the two parameters (u_*) and (b_*), then

$$F\left\{\frac{|\overline{cw}(0)|}{h\beta g|\theta w(0)|}\right\} = F\left\{\frac{u_*^2}{h\ b^*}\right\} = 0, \text{ or}$$

$$h = H^*\ L \tag{2.13}$$

where

$$L = u_*^2/b^* \tag{2.14}$$

and H^* is a constant of proportionality.

If the coriolis force is a significant component of the mean momentum budget, then (2.11) is replaced by

$$\frac{\partial \overline{cw}}{\partial z} = -\ ifC \ . \tag{2.15}$$

Adding the coriolis parameter ($f = 2\Omega \sin \phi$) to the dimensional analysis makes H* variable.

$$H^* = \frac{h}{L} = H^*\left(\frac{b_*}{u_* f}\right) \tag{2.16}$$

with a second dimensionless product ($b_*/u_* f$).

Using data from the NORPAC expedition, Kitaigorodsky found that equation (2.13) with a constant H* was insufficient for cases varying over more than twenty degrees of latitude (see Fig. 3).

Using Kitaigorodsky's data, it should be noticed that the Rossby number (Ro) based upon the layer depth and (u_*),

$$Ro = \frac{fh}{u_*} , \tag{2.17}$$

is less variant than H* = h/L for the same data. This can be seen in Figures 3 and 4.

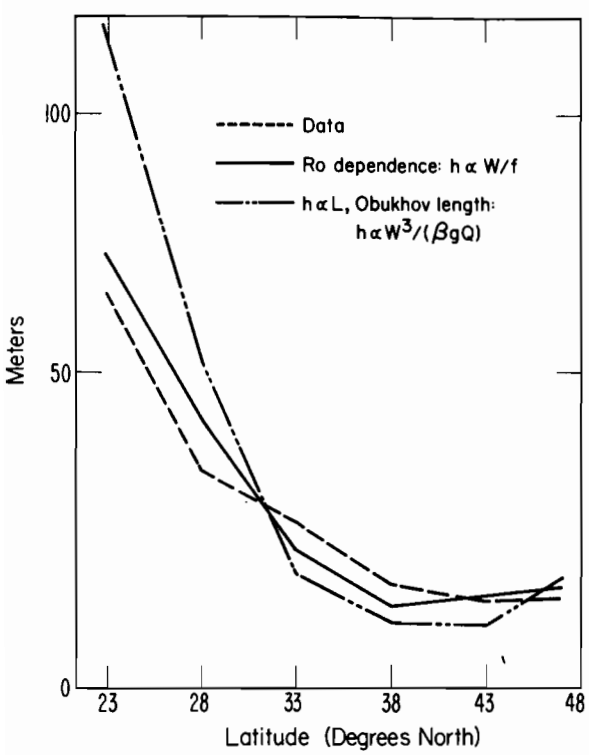

Figure 3. Mixed layer depth vs. latitude from Kitaigorodsky (1960).

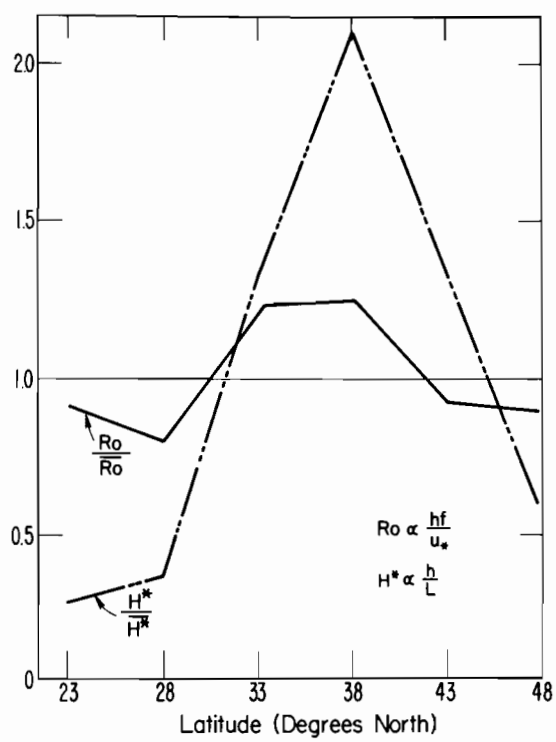

Figure 4. Mixed layer dependence upon both Ro^{-1} and H (data from Kitaigorodsky, 1960).*

There is a basic flaw in this model arising from the assumption that the ocean mixed layer is analogous to the "constant-flux" atmospheric surface layer. The ocean, in all probability, does have a surface layer over which fluxes are approximately constant and a quasi-steady state does exist. However, the depth of such a layer would be limited to at most the upper ten percent of the vertical extent of the entire mixed layer. With a constant heat flux at the surface, the mixed layer temperature and depth cannot both remain unchanged.

2.5 Compensation Depth for Shortwave Radiation

Kraus and Rooth (1961) also conceived a steady-state model based primarily upon the buoyancy equation. In their model however, steady state was made feasible by balancing the short wave radiation input $Q(z)$ with a net surface heat loss, $\rho_0 C_p \overline{\theta w}(0) > 0$, by means of evaporation, conduction, and infrared radiation. A compensation depth (h_c) is the depth at which a balance is struck between the surface heat loss, $\rho_0 C_p \overline{\theta w}(0)$, and the total radiation absorbed in the layer above,

$$\int_{-h_c}^{0} Q \, d z \, .$$

If

$$Q = \gamma \, Q_0 \, e^{\gamma z}$$

and if buoyancy is a function of temperature alone, then (1.11) becomes in steady state

$$0 = - \frac{\partial \, \overline{\theta w}}{\partial \, z} + \frac{Q}{\rho_0 c_p} \, . \qquad (2.19)$$

The depth ($z = - h_c$) is that level at which the turbulent flux $\overline{\theta w}$ goes to zero, with a stable temperature profile below and an unstable one above. Therefore in the region ($0 > z > - h_c$) turbulent kinetic energy can be convectively produced since here

$$\overline{bw} = \beta g \, \overline{\theta w} > 0 \, .$$

Integrating (2.19) from ($z = -h_c$) to ($z = 0$) and using (2.18) gives

$$h_c = \gamma^{-1} \ln\left(\frac{1}{1 - \rho C_p \overline{\theta w}(0)/Q_0}\right). \qquad (2.20)$$

Figure 5 is a schematic portrayal of the Kraus and Rooth concept. If

$$-\overline{\theta w} = K_H \frac{\partial T}{\partial z}, \quad K_H \sim \text{constant in } z, \qquad (2.21)$$

then (h_c) is also the depth of maximum temperature.

Using the eddy conductivity closure posed by (2.21), Kraus and Rooth examined the structure of the temperature field from the surface down through the mixed layer and across the interface, and its variation with changes in (Q) and the boundary conditions. Their solutions are only qualitatively useful because not only is (K_h) unknown, but also it is assumed to be constant--even across the density interface.

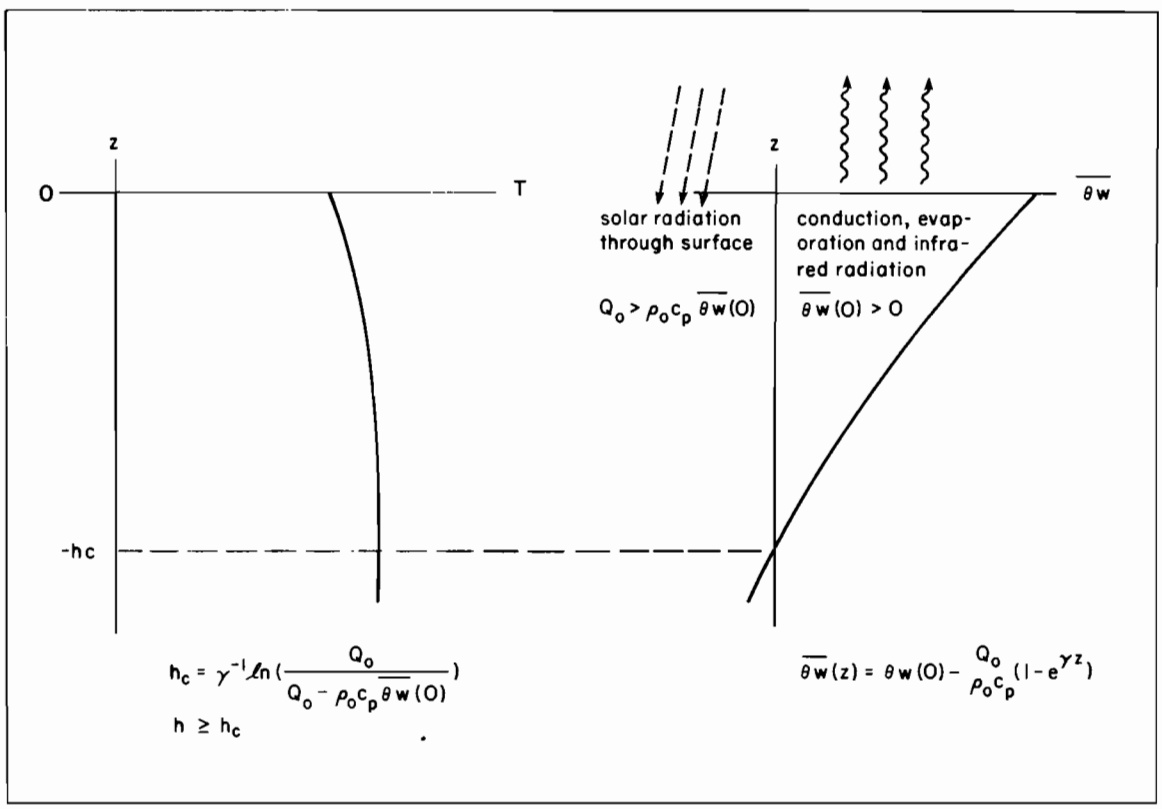

Figure 5. Effect of the compensation depth, h_c, assuming steady state and $Q = \gamma Q_0 e^{\gamma z}$.

With regard to the depth of the mixed layer (h), all they could really say was it must reach some depth greater than (h_c). "Dependent upon the intensity of the convective and wind drive turbulence, this convective regime may penetrate more or less deeply beyond the level (h_c)."

They visualized a steady-state layer depth as being possible only by requiring upwelling (W>o) of sufficient magnitude to maintain the vertical position of the entraining interface.

2.6 Prototype Turbulent-Energy-Budget Model: Kraus and Turner

Recognizing the limitations in application of the Kraus and Rooth model--no provision for a possible downward surface heat flux, no account of mechanical production of turbulent kinetic energy, and the steady-state constraint--Kraus and Turner (1967) further improved and generalized this kind of one-dimensional model. Their model was the first instance in which it was recognized that the budgets for thermal and mechanical energies could be considered separately. This is valid because the dissipative rate of heating ($\rho_0/J \cdot \varepsilon$) is several orders of magnitude smaller than either Q(z) or $|\rho_0 C_p \, \partial\theta w/\partial z|$. Therefore, their model consisted of two separate equations--the heat equation and a mechanical energy equation in which the net effect of the work of the wind on the sea surface and the viscous dissipation within the mixed layer are parameterized. This use of a mechanical energy equation together with the buoyancy (heat) equation and the boundary condition (1.23),

$$- \overline{bw}\,(-h) = \Delta B \, \frac{dh}{dt} \, , \tag{1.23}$$

gave for the first time a closed set of equations whose solution provided h(t).

If buoyancy is a function of temperature alone and constant in the mixed layer, equation (1.25) is applicable. Using the radiation absorption function (2.18) it becomes

$$h \, \frac{d\langle \overline{T} \rangle}{dt} + \Delta T \, \frac{dh}{dt} \, \Lambda = \frac{Q_0}{\rho_0 C_p} \, (1 - e^{-\gamma h}) - \overline{\theta w}\,(0) \, . \tag{2.22}$$

The turbulent kinetic energy equation, integrated from the top of the entrainment zone (z = - h) to the surface is

$$G - D = -\beta g \int_{-h}^{0} \overline{\theta w} \, dz \tag{2.23}$$

where $$G = -\int_{-h}^{0} \overline{u_i w} \frac{\partial U_i}{\partial z}\, dz$$

is the total rate of mechanical production and

$$D = \int_{-h}^{0} \varepsilon dz$$

is the total rate of dissipation within the mixed layer. Neither of these parameters in the Kraus-Turner model is an implicit variable, and each must be specified externally. The heat equation that leads to (2.22) is also used to eliminate $\overline{\theta w}$ from (2.23) by integrating between z and 0:

$$\int_{z}^{0} \left(\frac{d\langle \overline{T} \rangle}{dt} + \frac{\partial \overline{\theta w}}{\partial z'} - \frac{Q}{\rho_0 C_p} \right) dz' = 0 \text{ , or}$$

$$\overline{\theta w}\,(z) = \frac{-Q_0}{\rho_0 C_p} (1 - e^{\gamma z}) + \overline{\theta w}\,(0) - z \frac{d\langle \overline{T} \rangle}{dt} . \qquad (2.24)$$

Integrating $\overline{\theta w}$ (z) as prescribed by (2.24) from (z = - h) to (z = 0) gives

$$\int_{-h}^{0} \overline{\theta w}\, dz = \frac{1}{2} h^2 \frac{d\langle \overline{T} \rangle}{dt} - \left[\frac{Q_0}{\rho_0 C_p} - \overline{\theta w}(0) \right] h + \frac{Q_0}{\gamma \rho_0 C_p} \left[1 - e^{-\gamma h} \right]. \qquad (2.25)$$

Neglecting $e^{-\gamma h}$, equations (2.22), (2.23) and (2.25) can be used to give another equation (2.26), which together with (2.22) constitutes a closed system in h(t) and $\langle T \rangle$ (t) where G, D, Q_0 and $\overline{\theta w}(0)$ are prescribed functions of time at most.

$$\frac{h^2}{2} \frac{d\langle \overline{T} \rangle}{dt} + \Delta T h \frac{dh}{dt} \Lambda = \frac{G - D}{\beta g} + \frac{Q_0}{\rho_0 C_p \gamma} . \qquad (2.26)$$

An important contribution by Kraus and Turner was the conceptualization of a model for which a stationary or even retreating mixed layer depth is possible. In such a case where

$$\frac{dh}{dt} \leq 0, \quad \wedge \left(\frac{dh}{dt}\right) = 0 ,$$

equations (2.22) and (2.26) are still applicable because of the presence of the Heaviside unit step function. Setting ($h = h_r$) in the case of a retreating or steady mixed layer depth, these equations reduce to (2.22a) and (2.26a).

$$h_r \frac{d\langle\overline{T}\rangle}{dt} = \frac{Q_0}{\rho_0 C_p} (1 - e^{-\gamma h_r}) - \overline{\theta w}\,(0). \tag{2.22a}$$

$$\frac{h_r^2}{2} \frac{d\langle\overline{T}\rangle}{dt} = \frac{G - D}{\beta g} + \frac{Q_0}{\rho_0 C_p \gamma} . \tag{2.26a}$$

Neglecting short-wave radiation that escapes the mixed region and eliminating ($d\langle\overline{T}\rangle/dt$) between (2.22a) and (2.26a) gives

$$h_r = \frac{2(G - D)}{\beta g\,(Q_0 - \overline{\theta w}(0))} . \tag{2.27}$$

Whenever the surface boundary conditions and/or solar radiation adjust to make ($h_r < h$) the mixed layer will "retreat." Of course, the region does not unmix, in accordance with the second law of thermodynamics. The net rate of production of turbulent kinetic energy, G-D, is insufficient to balance the rate of increase of potential energy,

$$\int_{-h}^{0} - \beta g\, \overline{\theta w}\, dz,$$

required to mix the region all the way to the density interface. Consequently, as the region warms (notice that $d\langle\overline{T}\rangle/dt$ can be only positive at this time), a new density interface is established at $z = - h_r$.

Kraus and Turner model G in terms of the friction velocity:

$$G = u_*^3 . \tag{2.28}$$

Not knowing the importance of the viscous rate of dissipation,

$$D = \int_{-h}^{0} \varepsilon dz,$$

they simply neglect it. They find, however, that their model predicts a too-large value for (h), and that the dissipation should possibly be included.

Turner (1969) felt that there was a problem with (2.28) as well. From examination of observations of sudden wind speed increase and ensuing mixed layer deepening, he deduced that "a substantial fraction of the part of the work done by the wind which goes into the drift current is eventually used to deepen the surface layer." This statement reflects the need for a more comprehensive model, particularly for unsteady situations. Such a model should reflect the input of energy into the mean velocity profile and the time delay needed to shift some of this energy to turbulence.

Again with regard to the Kraus and Turner model, the setting of (D = 0) so that

$$- \beta g \int_{-h}^{0} \overline{\theta w}\, dz = G \qquad (2.29)$$

places an unrealistic constraint upon the buoyancy term: it becomes dependent only upon the mechanical production. The error in this is most obvious when there is strong surface cooling and

$$(- \int_{-h}^{0} \overline{\theta w}\, dz)$$

is less than zero.

Kraus and Turner also neglect the effect of entrainment in their turbulent kinetic energy budget, equation (2.23).

In spite of these deficiencies, this model was a big step in the right direction in its consideration of the turbulent energy budget in recognition of the energy source for mixing and entraining.

2.7 Adding Dissipation

Miropol'skiy (1970) and later Denman (1973a) assume that dissipation is a fixed fraction of the shear production, equation (2.30).

$$D = \delta' G \qquad (2.30)$$

where δ' is an empirical parameter to be determined from observations. This gives, instead of (2.29), the equation (2.31):

$$- \beta g \int_{-h}^{0} \overline{\theta w}\, dz = (1 - \delta') G \quad . \tag{2.31}$$

This does not solve the dissipation problem because δ' cannot have a constant value. In essence, dissipation must be allowed to adjust to the total situation as it evolves.

Miropol'skiy also assumed that $G \propto u_*^3$, but a variation of an exercise he uses to deduce this demonstrates perhaps the major source of error in a model like (2.28).

$$G = - \int_{-h}^{0} \left(\overline{uw}\, \frac{\partial U}{\partial z} + \overline{vw}\, \frac{\partial V}{\partial z} \right) dz \quad .$$

If $\partial \overline{uw}/\partial z = - fV$ and $\partial \overline{vw}/\partial z = fU$, then

$$G = \left[- \overline{uw}\, V - \overline{uw}\, V \right]_{-h}^{0} \sim u_*^3 \quad .$$

In general, however,

$$\frac{\partial \overline{uw}}{\partial z} = - fV - \frac{\partial U}{\partial t} \quad , \text{ and}$$

$$\frac{\partial \overline{vw}}{\partial z} = fU - \frac{\partial V}{\partial t} \quad , \text{ giving}$$

$$G = \left[- \overline{uw}\, U - \overline{vw}\, V \right]_{-h}^{0} - \int_{-h}^{0} \frac{\partial}{\partial t} \left(\frac{U^2 + V^2}{2} \right) dz \tag{2.32}$$

and thus indicating the importance of the mean kinetic energy and its distribution within the mixed layer. As will be shown, even if the wind is steady for long periods of time, the mean kinetic energy can change markedly on a time scale corresponding to the inertial period.

Most recently, the trend in the literature has been to model the mixed layer as a vertically homogeneous moving slab with density and velocity discontinuities at the entraining interface. Geisler and Kraus (1969) were the first to use the slab approach in their model of the atmospheric boundary

layer. This problem is almost completely analogous to the oceanic mixed layer problem except that the atmospheric boundary layer is driven by a horizontal pressure gradient rather than by a surface stress. A rigid surface boundary rather than a free surface also results in a subtle but important difference. Nevertheless, the basic setups of the two problems are the same.

Simultaneous calculation of the mean velocity together with (h) and (T) permits the implicit calculation of the mechanical production of turbulent energy, an improvement upon the previous (u_*^3) method.

The equations (2.33) and (2.34), reflecting the conservations of mean momentum and mean buoyancy are essentially the same as (1.24) and (1.25). The only real difference is that Geisler and Kraus assume a prescribed mean subsidence (analogous to ocean upwelling) in their atmospheric boundary layer. This non-zero vertical velocity (W) can result in a stationary mixed layer depth even when entrainment is occurring. This then is a different mechanism than that developed by Kraus and Rooth (1961) for obtaining a constant (h).

$$h \frac{d\langle C\rangle}{dt} + \Delta C \left(\frac{dh}{dt} - W\right) = - ifh \left(\langle C\rangle - Cg\right) - \overline{cw}\,(0) \; . \tag{2.33}$$

$$h \frac{d\langle \overline{T}\rangle}{dt} + \Delta T \left(\frac{dh}{dt} - W\right) = - \overline{\theta w}\,(0) \; . \tag{2.34}$$

In (2.33), $(- ifC_g)$ is the kinematic geostrophic pressure gradient, the source of momentum. The kinematic surface stress, $\overline{cw}\,(0)$ is a momentum sink in this case.

Geisler and Kraus seem to avoid the problem of dealing with the viscous dissipation of turbulent kinetic energy by prescribing a fixed value for the integrated flux Richardson number, Rf_I.

$$Rf_I = \frac{\int_0^h \overline{bw}\, dz}{\int_0^h \left(\overline{uw}\,\frac{\partial U}{\partial z} + \overline{uw}\,\frac{\partial V}{\partial z}\right) dz} \equiv n, \text{ constant} \; . \tag{2.35}$$

This, however, is equivalent to Miropol'skiy's method. From (2.31) and (2.35),

$$n = 1 - \delta' \; . \tag{2.36}$$

Since (n) is always a fixed positive number, and with no radiation absorption in the model, the buoyancy flux (heat flux) can only be downward. Therefore, this model like that of Kitaigorodsky is restricted in application to only those cases where the mixed layer is stable throughout.

2.8 Role of Mean Kinetic Energy

Pollard, Rhines and Thompson (1973) apply the slab approach to the oceanic mixed layer, but they complete the entrainment problem with a different mechanical energy requirement. The time rate of change of the total mean mechanical energy, potential plus kinetic, of the slab is set equal to the rate of work by the wind on the mean flow:

$$\frac{\partial \overline{PE}}{\partial t} + \frac{\partial \overline{KE}}{\partial t} = \left[- U \overline{uw} - V \overline{uw} \right]_{z=0} . \qquad (2.37)$$

This is the same as (1.12) integrated from ($z = - h - \delta$) to the surface if viscous dissipation is neglected and (U) and (V) are constant in (z) within the mixed layer. The turbulent buoyancy flux ($\overline{bw}$) gives the potential energy change using equation (1.11):

$$\frac{\partial \overline{PE}}{\partial t} = - \int_{-h}^{0} \overline{bw} \, dz = \frac{1}{2} h^2 \frac{\partial B}{\partial t} + h \, \Delta B \frac{\partial h}{\partial t} .$$

Neglecting the time rate of change of the turbulent kinetic energy,

$$\frac{\partial \overline{KE}}{\partial t} = \frac{1}{2} \frac{\partial}{\partial t} \left[(U^2 + V^2) h \right] .$$

If radiative heating is ignored, (2.37) reduces to

$$Ri^{*} = \frac{h \Delta B}{U^2 + V^2} = 1 . \qquad (2.37a)$$

Pollard, Rhines and Thompson assume that (2.37) applies as long as

$$\frac{\vec{\tau}}{\rho_0} \cdot \vec{U} \, (z = 0) = \left[- U \overline{uw} - V \overline{uw} \right]_0$$

is positive. As soon as this rate of work by the wind becomes negative, "energy flow to increase (h) ceases and since the water cannot unmix, (h) must be constant...". Therefore, mixed layer deepening would occur only up until one-half of an inertial period following the onset of a steady wind stress. This result is demonstrated by setting $\overline{cw}$ (0) = $- u_*^2$ and $\Delta C = \langle C \rangle$ in equation (1.24), giving

$$\frac{d(\langle C \rangle h)}{dt} + if \, (\langle C \rangle h) = u_*^2 .$$

The particular solution is $\langle U \rangle + i \langle V \rangle = (iu_*^2/fh)(e^{-ift} - 1)$. Hence $\vec{\tau} \cdot \vec{U}$ ($z = 0$) goes to zero when $\langle U \rangle$ vanishes at time $t = \pi/f$.

In this model, energy for entrainment is derived directly from the mean flow. A separate budget for turbulent energy is not considered. That is to say, the intensity of the turbulence is not considered to have an active role in the mechanism of entrainment in this model.

In a three-layer model of the ocean mixed layer, Niiler (1974) combined elements of Pollard et al. and Kraus and Turner (1967) in that both turbulent kinetic energy and the mean kinetic energy are considered to be important in the mechanism that determines rate of entrainment. Figure 6 is a diagram of the vertical temperature and velocity structures in this model. The turbulently active region was divided into three subregions: (i) a constant-flux surface layer, (ii) the major part of the whole region, and (iii) the entrainment zone, lying just above a "quiescent abyss."

The momentum and buoyancy equations used by Niiler are virtually the same as the "slab" equations (1.24) and (1.25) if $B = B(T)$ only.

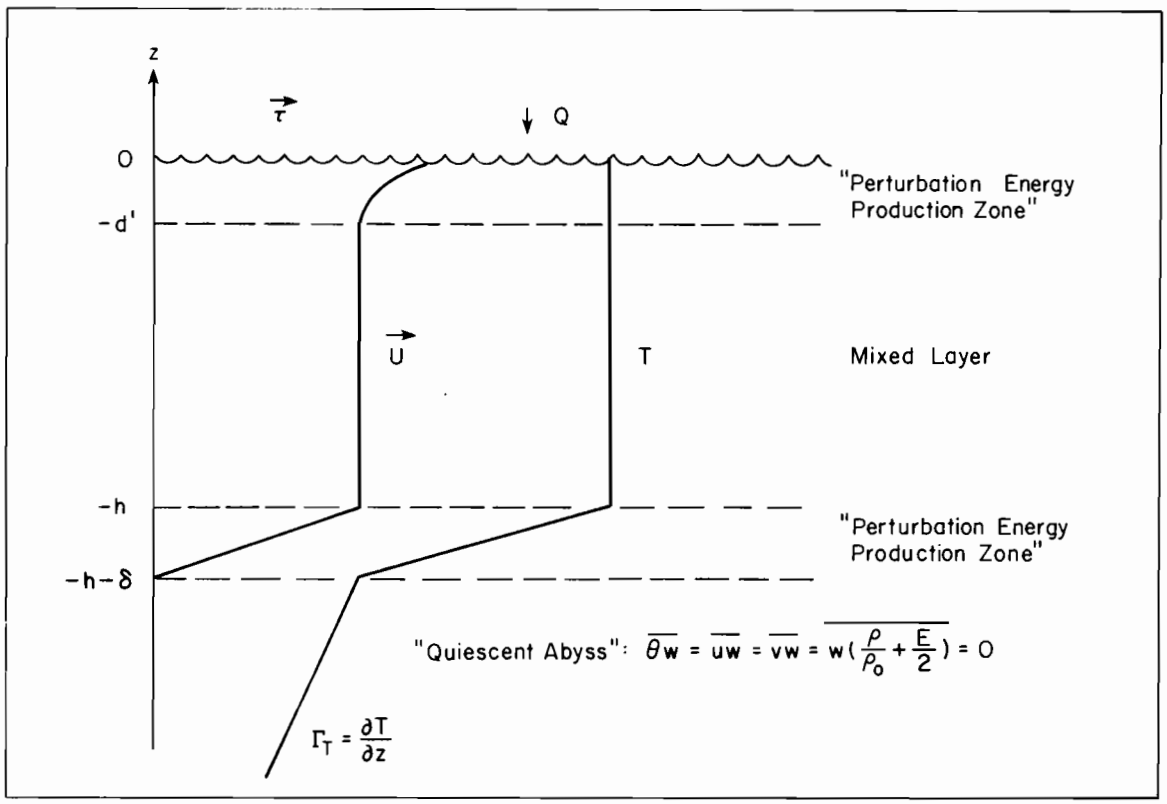

Figure 6. Idealized picture of ocean mixed layer (Niiler, 1974).

$$h \frac{d\langle C\rangle}{dt} + \Lambda \Delta C \frac{dh}{dt} = ifh \langle C\rangle - \overline{cw}(0) - \frac{F}{\rho_0} . \tag{2.38}$$

$$h \frac{d\langle \overline{T}\rangle}{dt} = \Lambda \Delta T \frac{dh}{dt} = - \overline{\theta w}(0). \tag{2.39}$$

Radiation absorption was assumed to occur entirely in the uppermost layer and was therefore included in $\overline{\theta w}(0)$. The additional term (F/ρ_0) is a "damping" force for inertial motions

$$\frac{F}{\rho_0} \propto |C| \, C \, h \tag{2.40}$$

within the mixed layer and presumably is related to the "'dissipation' of mean motions as well as the radiation flux of momentum from the bottom of the mixed layer." Pollard and Millard (1970) considered such a term as well, but one that was linear and thus resulting in an exponential damping. The time constant (τ_I) ranged from four to twenty-five inertial periods, depending upon the size of the inertial circle relative to the horizontal scale of the forcing wind system.

$$\tau_I = \frac{Ch\rho_0}{F} .$$

If the mean velocity below the density interface is zero and the mean temperature below the interface is given by $T(z < -h) = \Gamma_T z$, then the fluxes at $(z = -h)$ reduce to

$$- \overline{cw}(-h) = \Delta C \frac{dh}{dt} = \langle C\rangle \frac{dh}{dt} \tag{2.41}$$

and

$$- \overline{\theta w}(-h) = \Delta T \frac{dh}{dt} = (\langle T\rangle + \Gamma_T h) \frac{dh}{dt} . \tag{2.42}$$

Since $T = \langle T\rangle$ and $C = \langle C\rangle$ for the bulk of the mixed layer, the turbulent fluxes are linear functions in (z):

$$- \overline{cw}(z) = - \overline{cw}(0) - \frac{z}{h} \left[\overline{cw}(0) + \langle C\rangle \frac{dh}{dt} \right] . \tag{2.43}$$

$$- \overline{\theta w}(z) = - \overline{\theta w}(0) - \frac{z}{h} \left[\overline{\theta w}(0) + (\langle T\rangle + \Gamma_T h) \frac{dh}{dt} \right] . \tag{2.44}$$

The relative importance of the terms of the turbulent kinetic energy budget (1.13), was hypothesized to vary with subregion.

$$\frac{1}{2}\frac{\partial \overline{E}}{\partial t} = -\frac{\partial}{\partial z}\left[\overline{w\left(\frac{E}{2}+\frac{p}{\rho_0}\right)}\right] - \left[\overline{uw}\frac{\partial U}{\partial z} + \overline{vw}\frac{\partial V}{\partial z}\right] + \left[\overline{bw}\right] - \left[\varepsilon\right]. \quad (1.13)$$

The rate of mechanical production, $-\overline{u_i w}\,\partial U_i/\partial z$, was assumed to be non-zero only in the surface and entrainment subregions. In these two regions of small vertical extent, the buoyant damping was considered by Niiler to be insignificant. Thus the balance is between mechanical production, turbulent and pressure diffusion, and dissipation, equation (2.45a):

$$\frac{\partial}{\partial z}\left[\overline{w\left(\frac{p}{\rho_0}+\frac{E}{2}\right)}\right] \overline{uw}\frac{\partial U}{\partial z} + \overline{vw}\frac{\partial V}{\partial z} + \varepsilon = 0 \quad \text{for} \quad \left\{\begin{array}{l} 0 > z > -d' \\ -h > z > -h-\delta \end{array}\right\}. \quad (2.45a)$$

In this model $\partial U/\partial z = \partial V/\partial z = 0$ within the central part of the mixed region, and hence mechanical production is necessarily assumed to be zero. Therefore, here the buoyant damping and viscous dissipation are balanced by diffusion from the two adjacent production layers, giving equation (2.45b).

$$\frac{\partial}{\partial z}\left[\overline{w\left(\frac{E}{2}+\frac{p}{\rho_0}\right)}\right] - \overline{bw} + \varepsilon = 0 \quad \text{for } \{-d' > z > -h\} \quad . \quad (2.45b)$$

Integrating equations (2.45a) and (2.45b) vertically and combining them to eliminate $\overline{w(E/2 + p/\rho_0)}$ at $(z = -d')$ and $(z = -h)$ gives

$$-\left[\overline{w\left(\frac{p}{\rho_0}+\frac{E}{2}\right)}\right]_0 - \int_{-d}^{0}\left(\overline{uw}\frac{\partial U}{\partial z} + \overline{vw}\frac{\partial V}{\partial z}\right)dz - \int_{-d}^{0}\varepsilon\, dz$$

$$+ \frac{|\langle C\rangle|^2}{2}\frac{dh}{dt} = -\int_{-h}^{0}\overline{bw}\, dz \; . \quad (2.46)$$

In the manner of Kraus and Turner, Niiler parameterized the sum of the first three terms of (2.46) in terms of the surface stress.

$$-\left.\overline{w\left(\frac{p}{\rho_0}+\frac{E}{2}\right)}\right|_0 - \int_{-d}^{0}\overline{u_i w}\frac{\partial U_i}{dz}\, dz - \int_{-d}^{0}\varepsilon\, d\, z \equiv m_0\, u_*^3 \; . \quad (2.47)$$

Integrating (2.42) to give

$$-\int_{-h}^{0} \overline{bw}\, dz = -\beta g \int_{-h}^{0} \overline{\theta w}\, dz = \beta g \left[\frac{-\overline{\theta w}\,(0)\, h}{2} + \frac{h}{2} \left(\langle T \rangle + \Gamma_T h \right) \frac{dh}{dt} \right]$$

and using (2.47), equation (2.46) becomes

$$m_0 u_*^3 + \frac{|\langle C \rangle|^2}{2} \frac{dh}{dt} = \beta g \left[\frac{-\overline{\theta w}\,(0)\, h}{2} + \frac{h}{2} \left(\langle T \rangle + \Gamma_T h \right) \frac{dh}{dt} \right]. \qquad (2.48)$$

The system of equations (2.38), (2.39), and (2.48) is a closed set of equations in the three unknowns: - h, $\langle T \rangle$ and $\langle C \rangle$.

This model more resembles that of Kraus and Turner than it does that of Pollard et al because of the utilization of a parameterized turbulent kinetic energy equation rather than a total mechanical energy equation. The primary difference is the presence of the entrainment production term, $|\langle C \rangle|^2/2 \cdot dh/dt$, in (2.48) which necessitates the additional equation, the integrated momentum equation (2.38).

One aspect of important consequence in Niiler's model manifests the need for an even more comprehensive term-by-term modeling of the turbulent kinetic energy equation. This is the fact that the turbulent kinetic energy produced by entrainment, $|\langle C \rangle^2/2 \cdot dh/dt$, must go entirely toward increasing the potential energy. Because of the parameterization, (2.47), dissipation is not permitted to adjust to include either the direct effect of this particular source, or the less obvious effects related to the entrainment or lack of it.

The only solution to this predicament would seem to be to model dissipation separately from any of the source terms, allowing it to adjust to total turbulent intensity.

3. CLOSING THE PROBLEM

The equations (1.19a-c), (1.24), and (1.25) do not by themselves constitute a closed system of equations for the mixed layer. Vertical integration over the mixed layer simplified the equations but introduced yet another unknown, the mixed layer depth (h).

3.1 Net Viscous Dissipation in the Mixed Layer

$$\int_{-h-\delta}^{0} \varepsilon \, dz = \int_{-h-\delta}^{0} \nu \overline{\frac{\partial u_i}{\partial x_j} \frac{\partial u_i}{\partial x_j}} \, dz \quad .$$

A dissipation time scale (τ_ε) is defined by $\varepsilon \equiv \langle \overline{E} \rangle / \tau_\varepsilon$.

For fully-turbulent geophysical flows having large Reynolds numbers, viscous dissipation of the turbulence occurs primarily in the small eddies that are locally isotropic. As explained by Tennekes and Lumley (1972), an inviscid estimate of dissipation may be made by taking the rate at which large eddies supply energy to small eddies (equal to the rate of dissipation) to be proportional to the reciprocal of the time scale of the large eddies. If the time scale of these large eddies is proportional to the mixed layer depth divided by the rms turbulent velocity $\sqrt{\langle \overline{E} \rangle}$, then an integral model for dissipation in the mixed layer, independent of viscosity and the small scales is

$$\int_{-h-\delta}^{0} \varepsilon \, d \, z \equiv m_1 \langle E \rangle^{3/2} \tag{3.1}$$

where (m_1) is a constant of proportionality. For those situations where $\langle \overline{E} \rangle \propto u_*^2$, equation (3.1) is the same as that used by Miropol'skiy (1970) and Denman (1973).

An important concept in modeling dissipation is that of local isotropy. Turbulent kinetic energy generated at the largest scale ($\sim h$) is transferred without much additional production or dissipative loss through the inertial subrange to the larger and larger wave numbers (smaller eddies) by vortex stretching. Dissipation is significant only at the lower end of this inertial subrange.

Because there is no preservation of the original orientation, the small eddies of the inertial subrange are "locally isotropic." Therefore, dissipation draws approximately equally from all three turbulent energy components. Of course, the existence of an inertial subrange is dependent upon a large Reynolds number, and this is certainly the case for the oceanic mixed layer.

3.2 Net Effect of Redistribution of Turbulent Energy

$$R_\alpha = \int_{-h-\delta}^{0} \overline{\frac{p}{\rho_0} \frac{\partial u_\alpha}{\partial x_\alpha}} \, dz \quad .$$

As previously discussed, $R_1 + R_2 + R_3 = 0$, but R_α may be an important source of sink term for the individual turbulent kinetic energy budgets.

Following the early lead of Rotta (1951), but in agreement with the dominant term of the rational closure technique of Lumley and Khajeh-Nouri (1974),

$$R_\alpha \equiv -m_2 \sqrt{\langle \bar{E} \rangle} \quad (3 \overline{\langle u_\alpha^2 \rangle} - \langle \bar{E} \rangle) \ . \tag{3.2}$$

In addition to dimensional consistency, the concept leading to (3.2) is that of a "return to isotropy." In other words, the correlation of pressure and turbulent rate of strain tends to redistribute energy equally among the three components.

3.3 Shear Production

$$- \int_{-h-\delta}^{0} \left(\overline{uw} \frac{\partial U}{\partial z} + \overline{vw} \frac{\partial V}{\partial z} \right) dz \equiv u_*^2 \ |\delta C_0| + \frac{|\Delta C|^2}{2} \frac{dh}{dt} \tag{3.3}$$

where $|\delta C_0|$ is the "excess" surface mean velocity in the direction of the wind stress. Notice that in this instance the inhomogeneity of the mean velocity field cannot be neglected.

$$- \int_{-h-\delta}^{0} \left[\frac{\partial}{\partial z} \overline{w \left(\frac{p}{\rho_0} + \frac{E}{2} \right)} \right] d z \equiv m'_3 \ u_*^3$$

where $u_*^2 = |\overline{cw}\ (0)|$.

If $|\delta C_0|$ is proportional to (u_*), then (3.3) may be combined with the parameterized net input from breaking waves less loss to radiating internal waves:

$$G = \int_{-h-\delta}^{0} - \left[\overline{uw} \frac{\partial U}{\partial z} + \overline{vw} \frac{\partial V}{\partial z} + \frac{\partial}{\partial z} \left(\frac{\overline{wp}}{\rho_0} + \frac{\overline{wE}}{2} \right) \right] dz \equiv m_3 u_*^3 + \frac{|\Delta C|^2}{2} \frac{dh}{dt} \ . \tag{3.4}$$

This is basically in concurrence with the work of Kraus and Turner, Denman, and Niiler.

3.4 Need For an Entrainment Equation

Using the suggested relationship (1.24), (1.25), and (3.2), equations (1.14 a-c) become (3.5 a,b). The two horizontal component equations have been added together to give an equation for horizontal turbulent kinetic energy $\overline{\langle q^2 \rangle} = \overline{\langle u^2 \rangle} + \overline{\langle v^2 \rangle}$, together with the equation for vertical turbulent energy $\overline{\langle w^2 \rangle}$:

$$\frac{1}{2}\frac{d}{dt}\left(h\,\overline{\langle q^2\rangle}\right) = m_3 u^3 + \frac{|\Delta C^2|}{2}\frac{dh}{dt}\Lambda - m_2\sqrt{\langle \bar{E}\rangle}\left(\overline{\langle q^2\rangle} - \overline{2\langle w^2\rangle}\right) - \frac{2m_1}{3}\langle \bar{E}\rangle^{3/2}; \tag{3.5a}$$

$$\frac{1}{2}\frac{d}{dt}\left(h\overline{\langle w^2\rangle}\right) = \frac{h}{2}\left[\overline{bw}\,(0) - \Delta B\frac{dh}{dt}\Lambda - \frac{\beta g}{\rho_0 C_p}Q'\right] + m_2\sqrt{\langle \bar{E}\rangle}\left(\overline{\langle q^2\rangle} - 2\,\overline{\langle w^2\rangle}\right) - \frac{m_1}{3}\langle \bar{E}\rangle^{3/2}, \tag{3.5b}$$

where $Q' = -\int_{-h-\delta}^{0}\left(Q - \frac{2}{h}\int_{z}^{0} Q\,dz\right)dz$ and $\langle \bar{E}\rangle = \overline{\langle q^2\rangle} + \overline{\langle w^2\rangle}$.

If h (t) is unknown, equations (3.5a,b) together with (1.24) and (1.25) are an incomplete system of four equations in five unknowns: h, $\langle C\rangle$, $\langle B\rangle$, $\overline{\langle q^2\rangle}$. An entrainment hypothesis will provide the fifth equation needed to close the system.

4. ENTRAINMENT HYPOTHESIS

4.1 Entrainment in Earlier Mixed Layer Models

In this study the entrainment velocity, $u_e = dh/dt$, will be modeled explicitly in terms of the other free parameters of the system. However, in much of the literature treating models for the ocean mixed layer, (u_e) is a consequence of various assumed constraints placed upon the mechanical energy budget for the layer as a whole.

In the first really tenable model of the mixed layer that was capable of simulating a growing mixed-layer, Kraus and Turner (1967) assumed that all of the turbulent kinetic energy produced in the mixed layer goes to increase the potential energy of the system. After taking into account any surface

buoyancy flux, the balance of the potential energy change went to entrainment--mixing the requisite amount of underlying denser water uniformly throughout the homogeneous mixed region.

Their resultant entrainment velocity is

$$u_e = \frac{2\,(G - D) + \overline{wb}(0)h + \left(\frac{\beta g}{\rho_0 C_p}\right) Q' h}{h\Delta B} \tag{4.1}$$

where (G-D) is the net rate of mechanical production of turbulent kinetic energy minus the rate of viscous dissipation for the whole layer. The surface buoyancy flux $\overline{wb}(0)$ may either increase or decrease the entrainment velocity, depending upon its sign. Again, not knowing how to deal with the dissipation (D), Kraus and Turner ignored it. They set $G \equiv u_*^3$, so (4.1) becomes

$$u_e = \frac{2\,u_*^3 - u_* b_* h}{h\Delta B} \tag{4.1a}$$

where the solar heating function (Q') and the surface buoyancy flux have been combined in defining a buoyancy flux scale:

$$b_* = \frac{\frac{\beta g Q'}{\rho_0 C_p} - \overline{wb}\,(0)}{u_*} \tag{4.2}$$

Geisler and Kraus (1969), Miropol'skiy (1970), Denman (1973) and Niiler (1974) all assumed that a fixed fraction of the mechanical production of the turbulent kinetic energy would be dissipated. Therefore, their resultant entrainment rates are the same as (4.1a) except that some constant smaller than 2.0 would precede u_*^3.

Pollard, Rhines and Thompson (1973) did not explicitly consider the turbulent part of the mechanical energy budget, and therefore a conceptually different relationship results from their use of the total mechanical energy equation:

$$(h\Delta B - |\Delta C|^2)\,\frac{dh}{dt} = u_* b_* h\ . \tag{4.3}$$

If ($b_* = 0$) this reduces to Ri* = 1, or

$$h \geq \frac{|\Delta C|^2}{\Delta B} .$$

The ($\geq$) sign was added to prevent the mixed layer from retreating when mean kinetic energy is removed in the second half to the inertial cycle.

This approach at first seems to give a plausible result based upon the stability of the mean flow. The problem is that the mixed layer is already turbulent, and the system has an excess of turbulent kinetic energy, some of which may be available for mixing at the interface, regardless of the value of the overall Richardson number, Ri*. It is granted that Ri* may be constrained to having a value greater than some critical value by reason of a mean flow instability, but the fact is that in the laboratory and in geophysical cases, measurements indicate that entrainment occurs even though Ri* is much larger than one.

The entrainment experiments with mean shear of Kato and Phillips (1969) and Moore and Long (1971) (Figs. 7 and 8) show no direct relationship between Ri* and a maximum layer depth. More importantly, Turner (1968) and others have conducted experiments with growing mixed layers that had only turbulence and no mean shear (Ri* = ∞).

All of these laboratory results when examined together strongly imply that the bulk Richardson number Ri* is not the parameter most relevant to entrainment rate. Instead, a similar nondimensional number, using the turbulent kinetic energy (E) rather than $|\Delta C|^2$, is suggested.

As shown by Niiler (1974), the mean kinetic energy can influence entrainment rate by increasing (E) in a growing mixed layer. This in turn increases the average position of the bottom of an oceanic mixed layer undergoing a sequence of entrainment and retreat due to varying wind stress (u_*^2) and heating/cooling ($u_* b_*$) cycles. Figure 9 therefore indicates some statistical dependence upon the vertically-averaged Richardson number and hence Ri* as well.

4.2 Suggested Turbulent Mechanism

Benjamin (1963) shows that three basic types of instabilities are possible for a system where a flexible solid is coupled with a flowing fluid. At the interface between the mixed layer and the denser water beneath, a so-called class "A" instability will arise if

$$\Delta \tilde{u} \gtrsim \sqrt{\frac{\Delta B}{k}}$$

where (k) is the wave number of the interfacial disturbance,

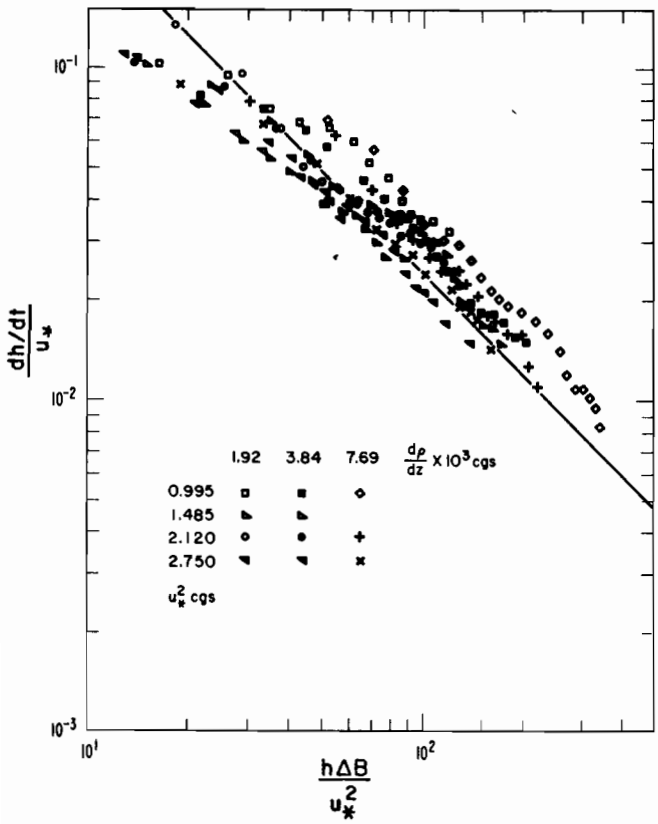

Figure 7. Rate of entrainment vs. $h\Delta B/u_*^2$ (Kato and Phillips, 1969). Figure taken from Kantha (1975).

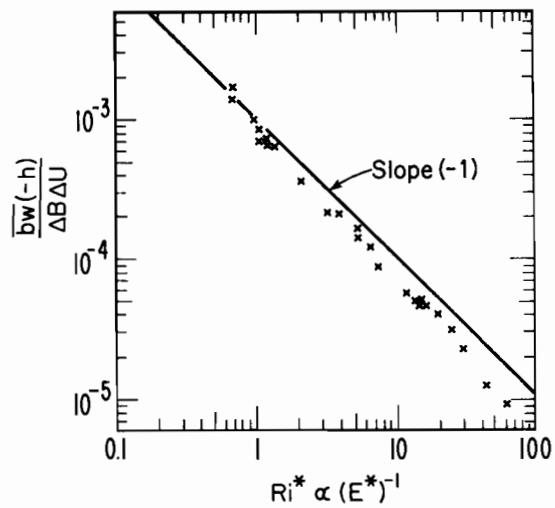

Figure 8. Rate of entrainment vs. Richardson number, from Moore and Long (1971) experiment.

$$\tilde{\eta} = \eta_0 \, e^{ik(x-c_1 t)} \, ,$$

and $(\Delta\tilde{u})$ is the total velocity change across the interface.

From Lamb (1932), §232, a class "C" instability, the Kelvin-Helmholtz instability, requires a higher $(\Delta\tilde{u})$.

$$\Delta\tilde{u} \gtrsim \sqrt{\frac{2\Delta B}{k}} \, .$$

However, the class "A" instability is dependent upon energy dissipation in the lower fluid, and this is likely to be small compared with inferred rates of convergence of energy flux, $-\partial/\partial z \, [\overline{w(p/\rho_0 + E/2)}]_{-h}$, at the interface. For geophysical flows of this type having large Reynolds and Péclet

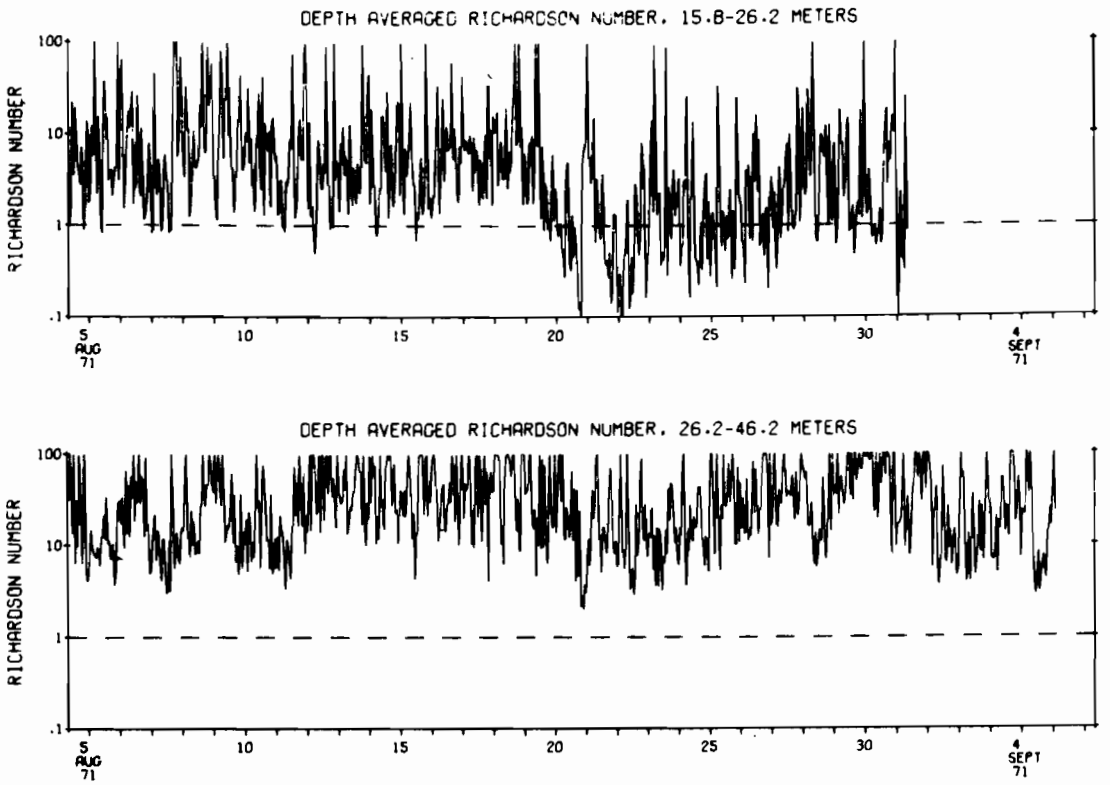

Figure 9. Depth-averaged gradient Richardson number, $\Delta z \Delta B / |\Delta C|^2$, versus time at two depth ranges (buoy measurements courtesy of David Halpern). Values greater than 100 were defined as equal to 100. Dashed horizontal line at 1.0 represents the condition for marginal dynamic stability.

numbers, the class "C" instability is therefore most likely to be the dominant mechanism leading to observed rates of entrainment.

The specific mechanism that is envisioned in the destabilization of the interface and the resulting entrainment is a "local" Kelvin-Helmholtz (K-H) instability. The shear needed to trigger such an instability is provided by the local turbulent eddies. The mean shear contributes to the instability but cannot in itself generate a critical Richardson number. The mean gradient Richardson number

$$Ri = \frac{\partial B/\partial z}{(\partial U/\partial z)^2} \tag{4.4}$$

would not be likely to achieve a critical value because the total instantaneous Richardson number,

$$Ri_T = \frac{\partial \tilde{b}/\partial z}{(\partial \tilde{u}/\partial z)^2} \tag{4.5}$$

is the relevant parameter. The minimum value of the envelope of $Ri_T(t)$ at the interface would determine the advent of any appreciable interface instabilities.

The onset of the K-H instability and its exponential growth rate is predicted by linear two-dimensional wave theory. As individual wave packets achieve a significant amplitude, the nonlinear and three-dimensional effects of the turbulence field prevail by distorting the wave shapes and advecting parts of the exposed cusps of denser water up into the mixed layer. Therefore, only the initial stages of the instability are strictly of the K-H type, where the induced suction at the crests of a perturbation wave on the interface is large enough to overcome the restoring buoyancy force.

4.3 Relevant Parameters and a Dimension Analysis

Since the mechanical energy needed to continue this mixing process and thus provide for a significant entrainment velocity must come from the turbulent eddies, the rate of supply of turbulent kinetic energy, $-\partial/\partial z\,[w(p/\rho_0 + E/2)]_{-h}$, just above the interface should determine the value of (u_e) for a given buoyancy jump (ΔB) and mean velocity drop $|\Delta C|$ across the interface.

As Long (1974) summarizes experimental studies, the nondimensional entrainment velocity W* is found to depend upon the first power of the dimensionless parameter E* based upon the buoyancy jump across the interface, the depth of the homogeneous layer (h), and the intensity of the turbulence $\langle\overline{E}\rangle$. Where Long assumes $\langle\overline{E}\rangle \alpha u_*^2$,

$$E^* = \frac{\langle\overline{E}\rangle}{h\Delta B} \tag{4.6}$$

and

$$W^* = \frac{u_e}{\sqrt{\langle\overline{E}\rangle}} \alpha E^* \,. \tag{4.7}$$

The relationship (4.7) together with an integrated turbulent kinetic energy equation to provide $\langle\overline{E}\rangle(t)$ plus the mean buoyancy equation could be used to close the problem.

The equation (4.7) is appealing because it depends strongly upon that which is accomplishing the erosion of the interface, the turbulent eddies having a length scale ($\sim h$) and velocity scale ($\sim \sqrt{\langle\overline{E}\rangle}$). However, its use based only upon laboratory evidence raises some questions about what is

really happening in the turbulent kinetic energy budget and why the mean velocity jump $|\Delta C|$ does not appear to be important at a first glance.

Resorting to a dimensional analysis in which the relevant parameters are

$$h,\ u_e,\ \Delta B,\ |\Delta C|,\ \text{and}\ \langle\overline{E}\rangle\ \text{gives}$$

$$\Psi\ (W^*,\ E^*,\ Ri^*) = 0 \qquad (4.8)$$

where

$$w^* = \frac{u_e}{\sqrt{\langle\overline{E}\rangle}}\ ,$$

$$E^* = \frac{\langle\overline{E}\rangle}{h\Delta B}\ ,$$

and

$$Ri^* = \frac{h\Delta B}{|\Delta C|^2}\ .$$

Here, the physical significance of (h) is its assumed proportionality to the length scale of the turbulent motion responsible for the interface instabilities.

Re-writing equation (4.8) so as to solve for (u_e),

$$u_e = \sqrt{\langle\overline{E}\rangle}\ \Psi'\left(\frac{\langle\overline{E}\rangle}{h\Delta B}\ ,\ \frac{h\Delta B}{|\Delta C|^2}\right)\ . \qquad (4.8a)$$

The experimental relationship (4.7) suggests that Ri* may be of negligible importance compared with E*. Other investigators besides Long, doing different experiments have found varying relationships between W* and E* (See Kantha, 1975).

The question of why W* would tend to be linearly related to E* in many but not all cases may be answered by closely examining the turbulent kinetic energy budget in the entrainment zone.

4.4 Turbulent Kinetic Energy Budget at the Density Interface and the Development of a Theoretical Equation for Turbulent Entrainment in the Presence of Mean Shear

At ($z = -h$), at the top of the entrainment zone and within the fully-turbulent mixing region, the turbulent kinetic energy equation is

$$0 = -\left[\overline{uw}\,\frac{\partial U}{\partial z} + \overline{vw}\,\frac{\partial V}{\partial z}\right]_{-h} + \left[\overline{bw}\right]_{-h} - \frac{\partial}{\partial z}\left[\overline{w\left(\frac{p}{\rho_{0_1}} + \frac{E}{2}\right)}\right]_{-h} - \left[\varepsilon\right]_{-h} . \quad (4.9)$$

At ($z = -h$), the turbulent fluxes are

$$\left[\overline{cw}\right]_{-h} = -\Delta C\,\frac{dh}{dt} \quad (4.10)$$

and

$$\left[\overline{bw}\right]_{-h} = -\Delta B\,\frac{dt}{dt} . \quad (4.11)$$

The convergence of flux of turbulent energy at the interface is responsible for the entrainment buoyancy flux, $\overline{bw}(-h)$.

$$\overline{bw}\,(-h) \simeq \frac{\partial}{\partial z}\left[\overline{w\left(\frac{p}{\rho_0} + \frac{E}{2}\right)}\right]_{-h} .$$

The problem is to estimate the time scale (τ_e) required to transport some of the turbulent energy $\langle\overline{E}\rangle$ to the vicinity of the entraining interface.

$$-\frac{\partial}{\partial z}\left[\overline{w\left(\frac{p}{\rho_0} + \frac{E}{2}\right)}\right]_{-h} = \frac{\langle\overline{E}\rangle}{\tau_e} .$$

The mixed layer depth (h) or a length scale proportional to (h) is the distance over which turbulent energy must be transported by the vertical component of turbulent velocity (w). Therefore, (τ_e) is taken to be proportional to (h) divided by the rms vertical velocity scale, $\sqrt{\langle\overline{w^2}\rangle}$, giving the entrainment hypothesis, equation (4.12). This equation is a refinement of what Tennekes (1973) has suggested. The difference is the use of $\sqrt{\langle\overline{w^2}\rangle}\,\langle\overline{E}\rangle$ rather than $\langle\overline{E}\rangle^{3/2}$.

$$- \frac{\partial}{\partial z} \left[\overline{w\left(\frac{p}{\rho_0} + \frac{E}{2}\right)} \right]_{-h} \equiv m_4 \frac{\sqrt{\langle \overline{w^2} \rangle \langle E \rangle}}{h} . \qquad (4.12)$$

Two possibilities are suggested for how the mean shear at the interface should adjust. The first is according to a gradient-diffusion model having an eddy viscosity scaling with the integral scales of the mixed-layer turbulence. The mean shear becomes

$$\frac{\partial C}{\partial z} \equiv - m_5 \frac{\overline{cw}}{h\sqrt{\langle \overline{w^2} \rangle}} . \qquad (4.13)$$

Then if local dissipation is negligible compared with the flux divergence at the interface, equation (4.9), using (4.10) - (4.13), becomes

$$\frac{m_5 \, |\Delta C|^2}{h \sqrt{\langle \overline{w^2} \rangle}} \left(\frac{dh}{dt}\right)^2 - \Delta B \left(\frac{dh}{dt}\right) + \frac{m_4 \sqrt{\langle \overline{w^2} \rangle} \, \langle \overline{E} \rangle}{h} = 0 . \qquad (4.14)$$

For those cases where $\langle \overline{w^2} \rangle$ is proportional to $\langle \overline{E} \rangle$, (4.14) can be reduced to simply

$$(W^*)^2 - \frac{Ri^*}{m_5'} - (W^*) + \frac{m_4'}{m_5'} E^* \, Ri^* = 0 \qquad (4.15)$$

in non-dimensional form. Solving (4.15) for W* gives

$$W^* = \frac{Ri^*}{2m_5'} - \sqrt{\left(\frac{Ri^*}{2m_5}\right)^2 - \frac{m_4'}{m_5'} E^* Ri^*} \qquad \text{or}$$

$$W^* = \frac{Ri^*}{2m_5'} \left[1 - \sqrt{1 - 4\phi^*} \right] \qquad (4.16)$$

where

$$\phi^* - m_4' \, m_5' \frac{E^*}{Ri^*} . \qquad (4.17)$$

If $\phi^* < \frac{1}{4}$, the binomial expansion gives

$$\sqrt{1 - 4\,\phi^*} = 1 - 2\,\phi^* - 2\,\phi^{*2} - 4\,\phi^{*3} - \ldots .$$

and therefore (4.16) may also be written as

$$W^* = m_4 E^* \left(1 + \phi^* + 2\,\phi^{*2} + \ldots .\right) . \qquad (4.16a)$$

For small ϕ^*, (4.16a) rapidly converges and only the first term may be needed. For more general applications, where $\langle \overline{w^2} \rangle$ is not always proportional to $\langle \overline{E} \rangle$, the equivalent solution to (4.14) is

$$\frac{dh}{dt} = \frac{m_4 \sqrt{\langle \overline{w^2} \rangle}\, \langle \overline{E} \rangle}{h \Delta B} \left[1 + \frac{m_4 m_5 \langle \overline{E} \rangle |\Delta C|^2}{(h \Delta B)^2} + \ldots . \right] . \qquad (4.18)$$

A second possible way for the mean shear at the interface to adjust is so as to maintain a gradient Richardson number of critical size, Ri_δ. Then in place of (4.13), the thickness of the interface (δ) adjusts so that

$$\left| \frac{\partial C}{\partial z} \right| - h \equiv \frac{\Delta B}{|\Delta C|} \frac{1}{Ri_\delta} \qquad (4.19)$$

where

$$Ri_\delta = \frac{\delta \Delta B}{|\Delta C|^2} . \qquad (4.20)$$

In this case, equation (4.9) becomes

$$-\left(1 - \frac{1}{Ri_\delta}\right) \Delta B \frac{dh}{dt} + m_4 \frac{\sqrt{\langle \overline{w^2} \rangle}\, \langle \overline{E} \rangle}{h} = 0 \qquad (4.21)$$

or

$$\frac{dh}{dt} = \frac{m_4'' \sqrt{\langle \overline{w^2} \rangle}\, \langle \overline{E} \rangle}{h \Delta B} \quad . \tag{4.21a}$$

If Ri_δ is a constant of order one, then (4.20) predicts, independent of the entrainment equation (4.21a),

$$\frac{\delta}{h} \simeq \frac{1}{Ri^*} \quad . \tag{4.22}$$

4.5 Comparison with Moore and Long (1971) Experiment

Figure 10 is a fit equation (4.16) to the results of Moore and Long (1971). The constants (m_4') and (m_5') are determined by the best fit. Notice that in this experiment $(E^*)^{-1}$ happens to be proportional to Ri^*. This is probably due to the experimental method and has no general significance for the ocean mixed layer. Also, W^* can be interpreted only as a dimensionless entrainment flux for this experiment because the experiment involves two turbulent mixed layers, each entraining the other equally, resulting in a motionless interface, giving

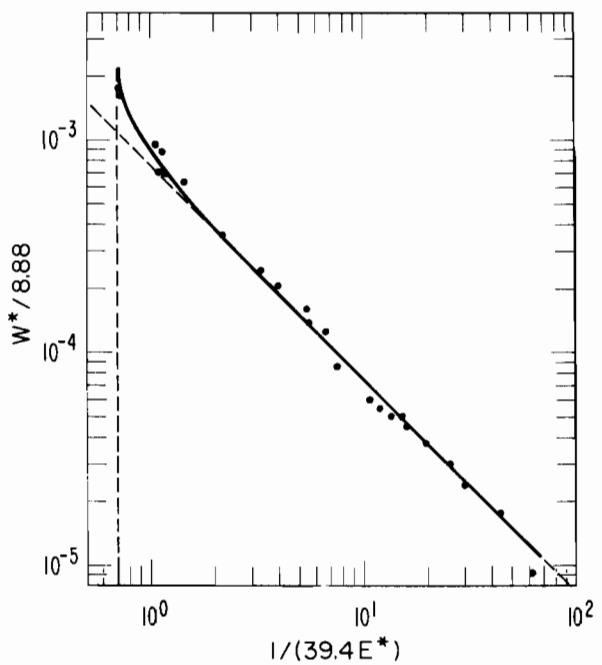

Figure 10. Theoretical entrainment curve vs. data of Moore and Long (1971). An instability is predicted at $E^*=0.036$. The slope approaches (-1) as E^* decreases.

$$W^* = \frac{-b\overline{w}(-h)}{\Delta B \sqrt{\langle \overline{E} \rangle}} = \frac{-u\overline{w}(-h)}{\Delta U \sqrt{\langle \overline{E} \rangle}} \ .$$

The lowest order term of (4.18) agrees with the general theory of Kraus and Turner (1967) and the experiment of Kato and Phillips (1969) for those instances where

$$\sqrt{\langle \overline{w^2} \rangle} \ \langle \overline{E} \rangle \sim m \ u_*^3 - u_* b_* h \ .$$

The higher order terms of (4.18) contribute to the entrainment process by a feedback mechanism that seems to explain the large-scale instability observed by Moore and Long for small Ri*. Equation (4.18) predicts an instability when $Ri^* \leq (Ri^*)_{cr}$

where
$$(Ri^*)_{cr} = 4 \ m_4 m_5 \frac{\langle \overline{E} \rangle}{h \Delta B} \ . \tag{4.23}$$

For the Moore-Long experiment, $(E^*/Ri^*)_{cr} = 0.105$, or

$$(Ri^*)_{cr} = 9.55 \frac{\langle \overline{E} \rangle}{h \Delta B} \ . \tag{4.23a}$$

Although this instability seems to be possible in the laboratory, it is not clear whether it can ever occur in the oceanic mixed layer because the expected turbulent entrainment attributable to the turbulent flux convergence (4.12) alone is sufficient to increase ($h\Delta B$) at a more rapid rate than Ri* may decrease.

The instability observed tends to verify the gradient-diffusion hypothesis, equation (4.13), at least for small Ri*. However, the constant $-Ri_\delta$ hypothesis, equation (4.19) seems to be a better fit for $\partial U/\partial z(-h)$ over most of the range of E*. Figure 11 is a plot of the observed (δ/h) versus the values predicted by equation (4.22).

Of course, the side walls in flume experiments of this type prohibit pushing the results too hard, but it is fairly clear that the Moore and Long experiment as well as the others mentioned verify the lowest order term of (4.18a) as well as (4.21a)--no matter how $\partial C/\partial z(-h)$ is modeled. Therefore this shall be taken as the entrainment equation:

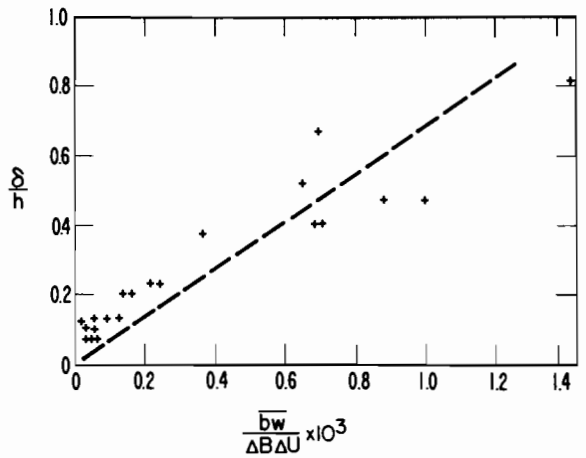

Figure 11. Predicted interface slope and Moore and Long measurements versus dimensionless buoyancy flux.

$$\frac{dh}{dt} = \frac{m_4 \sqrt{\langle \overline{w^2} \rangle} \ \langle \overline{E} \rangle}{h \Delta B} \quad . \tag{4.24}$$

4.6 Completed Model for Shallow Mixed Layers

Equations (1.24), (1.25), (3.5a,b) and (4.24) constitute a closed set of five equations in the five mixed-layer variables:

$$h \frac{d\langle C \rangle}{dt} = - \Delta C \frac{dh}{dt} \Lambda - \text{if } \langle C \rangle h - \overline{cw}(0) \ . \tag{1.24}$$

$$h \frac{d\langle B \rangle}{dt} = - \Delta B \frac{dh}{dt} \Lambda + \frac{\beta g}{\rho_0 C_p} \int_{-h-\delta}^{0} Q dz - \overline{bw}(0) \ . \tag{1.25}$$

$$\frac{1}{2} \frac{d}{dt} (h \langle \overline{q^2} \rangle) = m_3 u^3 + \frac{|\Delta C|^2}{2} \frac{dh}{dt} \Lambda - m_2 \sqrt{\langle \overline{E} \rangle} \ (\langle \overline{q^2} \rangle - 2 \langle \overline{w^2} \rangle) - \frac{2 m_1}{3} \langle \overline{E} \rangle^{3/2} \ . \tag{3.5a}$$

$$\frac{1}{2} \frac{d}{dt} (h \langle \overline{w^2} \rangle) = - \frac{h}{2} (u_* b_* + \Delta B \frac{dh}{dt} \Lambda) + m_2 \sqrt{\langle E \rangle} \ (\langle \overline{q^2} \rangle - 2 \langle \overline{w^2} \rangle) - \frac{m_1}{3} \langle \overline{E} \rangle^{3/2} \ . \tag{3.5b}$$

$$\frac{dh}{dt} = \frac{m_4 \sqrt{\langle \overline{w^2} \rangle} \ \langle \overline{E} \rangle}{h \Delta B} \quad . \tag{4.24}$$

In addition to $\underline{Q}(z,t)$, other specified (external) conditions are the surface fluxes $u_* b_*$ and $\overline{cw}(0)$.

Starting with initial conditions on $\langle C \rangle$, $\langle B \rangle$, $\langle \overline{q^2} \rangle$, $\langle \overline{w^2} \rangle$, and h, the model is solved as an initial-value problem in time.

Also to be specified separately are the initial profiles of B and C below the bottom of the mixed layer. These two variables contribute to ΔC and ΔB, which are important for a deepening mixed layer:

$$\Delta B = \langle B \rangle - B\,(-h - \delta)\ ; \tag{4.25}$$

$$\Delta C = \langle C \rangle - C\,(-h - \delta)\ . \tag{4.26}$$

5. BEHAVIOR OF THE EQUATIONS

5.1 Nondimensional Form of the Turbulent Energy and Entrainment Equations

Using the surface flux scales u_* and b_*, new dimensionless variables are defined:

$$H^* = \frac{u_* b_*\, h}{2 m_3\, u_*^3}\ ; \tag{5.1}$$

$$P^* = \frac{h \Delta B}{2 m_3 u_*^3} \frac{dh}{dt}\ ; \tag{5.2}$$

$$E^*_{ii} = \left(\frac{m_1}{m_3}\right)^{2/3} \frac{\langle \overline{E} \rangle}{u_*^2}\ ; \tag{5.3}$$

$$E^*_{33} = \left(\frac{m_1}{m_3}\right)^{2/3} \frac{\langle \overline{w^2} \rangle}{u_*^2}\ . \tag{5.4}$$

H^* is the ratio of buoyant damping (production) from surface heating (cooling) to wind-stress production. P^* is the ratio of energy lost by entrainment (potential energy increase) to wind-stress production.

Invoking the quasi-steady state assumption for the turbulent energy budget, the entrainment and turbulent energy equations become

$$P^* = \frac{p_1}{2} E^*_{ii} \sqrt{E^*_{33}} , \tag{5.5}$$

$$0 = 1 + \frac{P^*}{Ri^*} - p_2(E^*_{ii} - 3E_{33}) \sqrt{E^*_{ii}} - \frac{2}{3} (E^*_{ii})^{3/2} , \tag{5.6}$$

and $$0 = - H^* - P^* + p_2 (E^*_{ii} - 3E^*_{33}) \sqrt{E^*_{ii}} - \frac{1}{3} (E^*_{ii})^{3/2} , \tag{5.7}$$

where $$p_1 = \frac{m_4}{m_1} \text{ and } p_2 = \frac{m_2}{m_1} . \tag{5.8),(5.9}$$

5.2 Determination of the Constants

The ratio $m_2/m_1 = p_2$ is equivalent to $(18\ \ell_1/\Lambda)$ where (ℓ_1/Λ) is the redistribution to dissipation length scale ratio of Mellor and Herring (1973). From boundary layer data, they suggest

$$\frac{\ell_1}{\Lambda} = 0.05 \pm 0.01 .$$

Hence p_2 is of order one and will be taken to be equal to one in this analysis

$$p_2 = \frac{18\ell_1}{\Lambda} \simeq 1 . \tag{5.10}$$

The ratio $m_4/m_1 = p_1$ may be determined from the asymptotic case of pure convection, $H^* \to - \infty$ and $Ri^* = \infty$. The equations yield

$$p_1 = \left(\frac{r}{1-r}\right) \frac{2}{\sqrt{E^*_{33}/E^*_{ii}}} \tag{5.11}$$

where $$\frac{E^*_{33}}{E^*_{ii}} = \frac{1}{3} \left(1 + \frac{2}{3p_2}\right) \quad \text{for large } Ri^*. \tag{5.12}$$

The fraction (r) of turbulent energy converted to potential energy by entrainment is found to be 0.036 ± 0.031 by Farmer (1975) from measurements under the ice. Using $p_2 = 1$ and $r = 0.036$, equation (5.11) gives $(p_1 = 0.1)$.

P* may now be solved as a function of H* and Ri*. Figure 12 shows P* (H*) for Ri* = ∞ and Ri* = 1.

The one remaining constant needed to complete the model is m_3. This may be determined from the Kato and Phillips results, Figure 7, together with P*(H* = 0) from Figure 12.

$$P^*(0) = \frac{h\Delta B}{2m_3 u_*^3} \frac{dh}{dt} (b_* = 0) = 0.0227 \ . \tag{5.13}$$

$$h\Delta B \frac{dh}{dt} (b_* = 0) = 2.5 \ u_*^3 \ . \tag{5.14}$$

This gives $m_3 = 55$.

However, this value seems to be quite high for an oceanic mixed layer. The conceptual model for the mixed layer developed earlier, equation (3.3), implies that

$$m_3 = |\delta C_0|/u_*$$

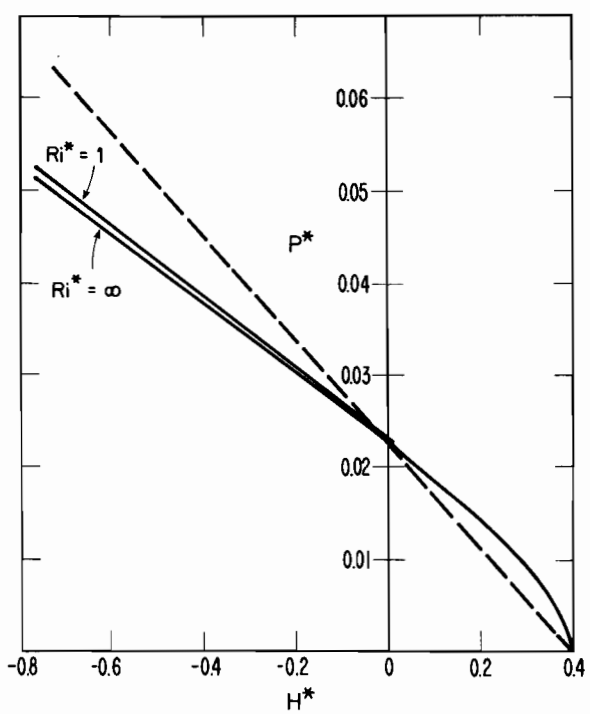

Figure 12. Model solution for shallow mixed layers: potential energy rate of increase due to entrainment versus layer stability.

where δC_0 is the excess surface and wind-drive current:

$$\delta C_0 = C\ (Z = 0) - \langle C \rangle\ .$$

A more moderate value of $m_3 \sim 10$ is expected. In the laboratory experiment, the production was enhanced by the side-wall boundary layers, resulting in a too-large value for m_3.

There is another method of determining (m_3) which is suggested by Figure 12. Rather than using neutral ($H^* = 0$) stability situations (storm situations are only approximately neutral by virtue of a large u_*^3 compared with $u_* b_* h$), cases of limiting strong stability where $P^* = 0$ and $h = h_r$ could be examined.

$$H^*_{max} = 0.4 = \frac{u_* b_* h}{2 m_3 u_*^3}\ , \text{ so}$$

$$m_3 = \frac{u_* b_* h}{0.8\ u_*^3}\ . \qquad (5.15)$$

The effective buoyancy flux $u_* b_*$, given by equation (4.2) should properly be determined by measuring $Q(Z)$, and the mixed layer depth $h = h_r$ should be ascertained to be in the "retreat mode": $dh/dt \leq 0$. This method remains to be attempted.

5.3 Comparison With Earlier Models

The dotted straight line in Figure 12 is equivalent to the solution for P^* (H^*) if equation (4.1a) is calibrated to behave properly for both the retreating ($H^* = H^*_{max}$) and neutral ($H^* = 0$) situations. The greatest difference between the two models then occurs as H^* becomes increasingly negative. This inability to calibrate the earlier model to both stable summer and convective fall situations has been demonstrated by Thompson (1974).

Nearly equivalent to the Kraus-Turner type model for entrainment, equation (4.1a), is Tennekes's model which suggests in effect that

$$P^* = \frac{p\hat{\imath}}{2}\ (E^*_{ii})^{3/2} \qquad (5.16)$$

rather than (5.5). In such a model, the total turbulent kinetic energy equation, the sum of (5.6) and (5.7) is used:

$$0 = 1 - H^* - \left(1 - \frac{1}{Ri^*}\right) P^* - (E_{ii}^*)^{3/2} \quad . \qquad (5.17)$$

The redistribution term does not appear at all in (5.17) but this very term is the source of an ambiguity as $H^* \rightarrow H^*_{max} = 1$. As H^* gets larger, E^*_{ii} and hence P^* go to zero for the set of equations (5.16) and (5.17). If rather than using (5.17), we consider the component equations together with (5.16), no unique solution exists for H^* when $P^* = 0$. Considering the budget for the vertical component only reveals that (H^*_{max}) must be less than one and that E^*_{ii} must be greater than zero when $P^* = 0$. This, however, violates (5.16). The alternative equation (5.5) does not have this problem and it suggests a more consistent mechanism for layer retreat.

As H^* approaches its maximum value, more and more of the vertical component of turbulence is damped. Notwithstanding the redistribution effect, eventually redistribution cannot keep up with the combined losses due to buoyant damping and viscous dissipation. Virtually all of the energetic large-scale turbulent motion is two-dimensional, and the vertical flux of turbulent energy $(-\overline{wE})$ into the interface ceases and therefore entrainment stops. If (b^*) is further increased (or u_* decreased), (h) must retreat since H^* cannot exceed $H^*_{max} \sim 0.4$. Locally, at the base of the mixed layer, this would correspond to the flux Richardson number (Rf) surpassing a critical magnitude ($\simeq 0.2$).

Summing up, a new mixed-layer bulk model has been proposed that suggests that the energy redistribution between vertical and horizontal components of turbulence must be accounted for in a general model used to treat the entire range of stability--from pure convection to layer retreat. The proportion of vertical turbulent energy to total turbulent kinetic energy, E^*_{33}/E^*_{ii} of Figure 13, varies most significantly in the typical oceanic range of possibilities, $H^* = 0.4$ to ~ -1.

Layer retreat is predicted to occur for a smaller value of stability than is required with the earlier models because viscous dissipation remains important as long as $u_* > 0$.

The model, as it stands, is incomplete. The above applies only to the relatively shallow boundary layer associated with summer conditions. An additional feature is required for year-round application of the model because of the importance of the rotational time scale in the physics of deep mixed layers.

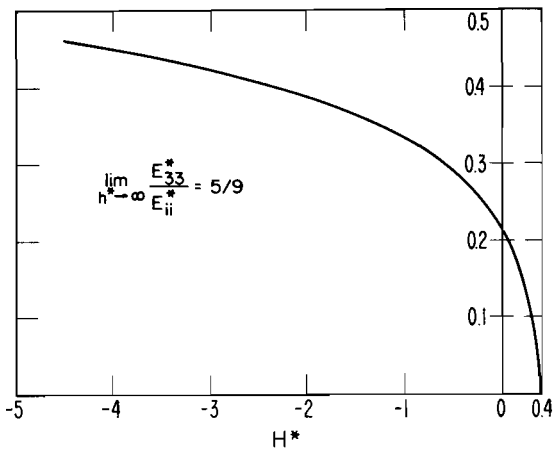

Figure 13. Ratio of vertical turbulent kinetic energy to total turbulent kinetic energy as a function.

6. DEEP MIXED LAYERS: LIMIT TO MAXIMUM DEPTH

6.1 Limiting Dissipation Time Scale

The need for a constraint upon the maximum depth of the mixed layer has been demonstrated. Niiler has pointed out that models of the Kraus-Turner type will continue to deepen incessantly during each winter cooling period. This is the unavoidable consequence of requiring some fraction of the net production of turbulent energy to be allotted to increasing the potential energy by means of entrainment.

Thompson (1974) also found this to be true. In doing a year-round integration, the model required an unrealistic value for mean annual surface heat flux yielding a net heat storage in order to achieve a realistic cycle.

Outside of the tropical latitudes and away from the continental shelves, lateral advection and upwelling are insufficient to balance this heat storage. The most noticeable failure of the model is at mid-latitude regions having a permanent pycnocline.

The model for dissipation is still

$$\varepsilon \sim \frac{\langle \overline{E} \rangle}{\tau_\varepsilon} \quad .$$

However, the dissipation time scale (τ_ε) was previously (in equation 3.1) governed by the depth of the mixed layer and the turbulent velocity scale, giving a strictly convective time scale:

$$\tau_\varepsilon \propto \frac{\ell_1}{\sqrt{\langle \overline{E} \rangle}} \sim \frac{h}{\sqrt{\langle \overline{E} \rangle}} \quad .$$

As planetary rotation begins to rotate the mean shear profile, and hence the geometrical aspects of the integral scale, there arises a new length scale, associated with the coriolis time scale (f^{-1}).

$$\ell_2 = \sqrt{\langle \overline{E} \rangle}\, f \ .$$

It is now increasingly clear from such studies as those by Arya and Wyngaard (1975) and Sundararajan (1975) that the coriolis time scale (f^{-1}) plays an important role in the internal structure of the convective planetary boundary layer or mixed layer. The concern here is more with the bulk properties of the region and less with the details within the mixed layer. However, it is suggested that this time scale has an important role in the overall turbulent energy budget above and beyond the turning and decay with depth of the mean velocity in the classic Ekman spiral. In reality the two effects are inseparable because of the link through local shear production.

Rather than to simply replace the convective scale (ℓ_1) by the rotational scale (ℓ_2), the suggestion is to use $\ell^{-1} = \ell_1^{-1} + \ell_2^{-1}$, giving equation (6.1),

$$\tau_\varepsilon^{-1} = \frac{\sqrt{\langle \overline{E} \rangle}}{h} + f. \tag{6.1}$$

Replacing (3.3) in the bulk (vertically integrated) formulation is equation (6.2)

$$\frac{\int_{-h}^{0} \varepsilon \, dz}{2 m_3 \, u_*^3} \equiv (E^*_{ii})^{3/2} + \acute{Ro}^{-1} \, (E^*_{ii}) \tag{6.2}$$

where

$$\acute{Ro}^{-1} = \left(\frac{m_1}{m_3}\right)^{1/3} \frac{fh}{u_*} \tag{6.3}$$

and, as before,

$$E^*_{ii} = \left(\frac{m_1}{m_3}\right)^{2/3} \frac{\langle \overline{E} \rangle}{u_*^2} \ .$$

6.2 Nondimensional Solution to the Entrainment Function

Equations (5.6) and (5.7) will now change to reflect the new term, giving (6.4) and (6.5).

$$0 = 1 + \frac{P^*}{Ri^*} - p_2 \left(E^*_{ii} - 3\, E^*_{33}\right) \sqrt{E^*_{ii}} - \frac{2}{3} E^*_{ii} \left(\sqrt{E^*_{ii}} + Ro^{-1}\right). \quad (6.4)$$

$$0 = - H^* - P^* + p_2 \left(E^*_{ii} - 3\, E^*_{33}\right) \sqrt{E^*_{ii}} - \frac{1}{3} E^*_{ii} \left(\sqrt{E^*_{ii}} + Ro^{-1}\right). \quad (6.5)$$

The entrainment equation, (5.5), remains unchanged.

$$P^* = \frac{p_1}{2} E^*_{ii} \sqrt{E^*_{33}} \,. \quad (5.5)$$

The solution to P^* is now a function of two variables, and is shown in

$$P^* = P^* \left(H^*, Ro^{-1}\right)$$

(Figure 14).

Specifically, several aspects concerning this nondimensional solution should be observed:

a. The solution for $Ro^{-1} = 0$ is identical with the earlier solution (Figure 12). This limit applies to both the case of shallow ($h << u_*/f$) mixed layer and the case of very low latitude, $\phi << u_*/|\Omega|h$.

b. For a retreating ($P^* = 0$) mixed layer, h_r is now a function of both the Rossby number and the stability H^*. Actually, h_r is uniquely determined by the product of these two parameters, making it a function of

$$B^* = \frac{b_*}{f u_*} \,.$$

A fairly good analytical approximation to this function is the hyperbolic relationship (6.6):

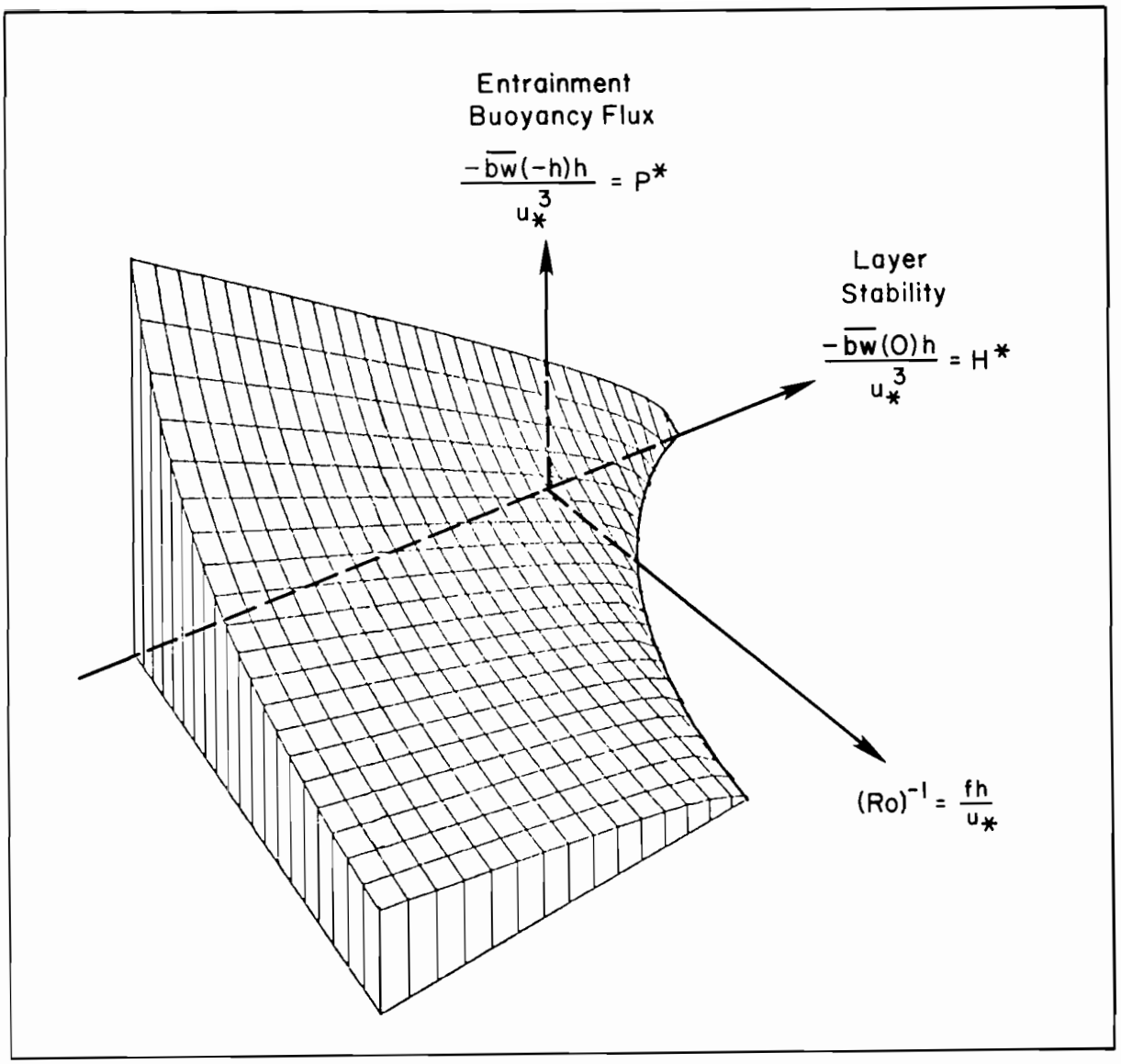

Figure 14. General solution to entrainment and turbulent kinetic energy equations.

$$(0.5 + H^*)\ \ (1.725 + Ro'^{-1}) = 1.552\ . \qquad (6.6)$$

which can be put in terms of h_r, giving equation (6.7).

$$h_r = \frac{1.725\ d' + 0.5L'}{2}\left(\sqrt{1 + \frac{2.76}{1.725\ d' + 5L'}} - 1\right) \qquad (6.7)$$

where d' is proportional to the Ekman depth of frictional resistance and L' is proportional to the Obukhov length scale.

The approximate solution for retreat, equation (6.7), has limiting cases of $d' \to \infty$ and $L' \to \infty$ that are in agreement with the earlier works of Kitaigorodsky (1960) and Rossby and Montgomery (1935).

$$L' = h_r/H^* \quad . \tag{6.8}$$

$$d' = h_r/Ro'^{-1} \quad . \tag{6.9}$$

Physically, the reason for the cessation of entrainment is ultimately the same for the convective boundary layer whether or not there is significant surface buoyancy flux. Dissipation that is approximately equally divided among the three components of the turbulent kinetic energy ($\overline{u^2} + \overline{v^2} + \overline{w^2}$) causes $\langle\overline{w^2}\rangle$ to be consumed more rapidly than it can be replaced by the pressure redistribution or "return to isotropy" effect. When this happens, the vertical flux of all properties, including the turbulence itself, ceases at the depth $h = h_r$. Buoyant damping or production modifies the overall budget, changing the relative value of $h_r f/u_*$, but dissipation plays the ultimate role.

Buoyant production may be sufficiently strong ($H^* < -0.5$) that dissipation cannot limit maximum mixed layer depth. Then the production of $\langle\overline{w^2}\rangle$ is too great to be overcome by dissipation with increasing depth.

c. A cyclical steady state is now possible. The surface buoyancy flux may go through an annual cycle having no net heat storage and $\langle h \rangle$ will not increase without bounds at the end of the cooling phase.

The simplest steady state is the neutral stability point represented by the coordinates (Ro'^{-1}, H^*, P^*) = (1.38,0.,0.). This is the situation for a neutral boundary layer, ($\overline{bw}(0) = 0$), where $h_r = 1.38\ d'$.

A simple cycle having a sinusoidal variation in $\overline{bw}(0)$ and a constant u_* is qualitatively depicted by Figure 15. This depicts the locus of coordinates for (Ro^{-1}, H^*) as the cycle progresses through a heating ($\overline{bw}(0) < 0$) and then a cooling ($\overline{bw}(0) > 0$) phase. The initial [0] and [4] points coincide at the neutral steady-state point. Between [0] and [1] buoyancy flux is directed downwards and is increasing, and the mixed layer retreats to its minimum depth which occurs at [1]. Between [1] and [2] there is active entrainment but the rate of entrainment is slow because of significant buoyant damping in the stable mixed layer. This would correspond to the summer warming period, culminating in maximum surface temperatures at about [2]. Cooling begins at [2] and reaches a maximum at [3]. Not until the end of the period does the rate of entrainment become significant because the heating period [0]- [2] causes a potential energy deficit in the system which must be replaced before deep-ending may proceed rapidly. In the time period just

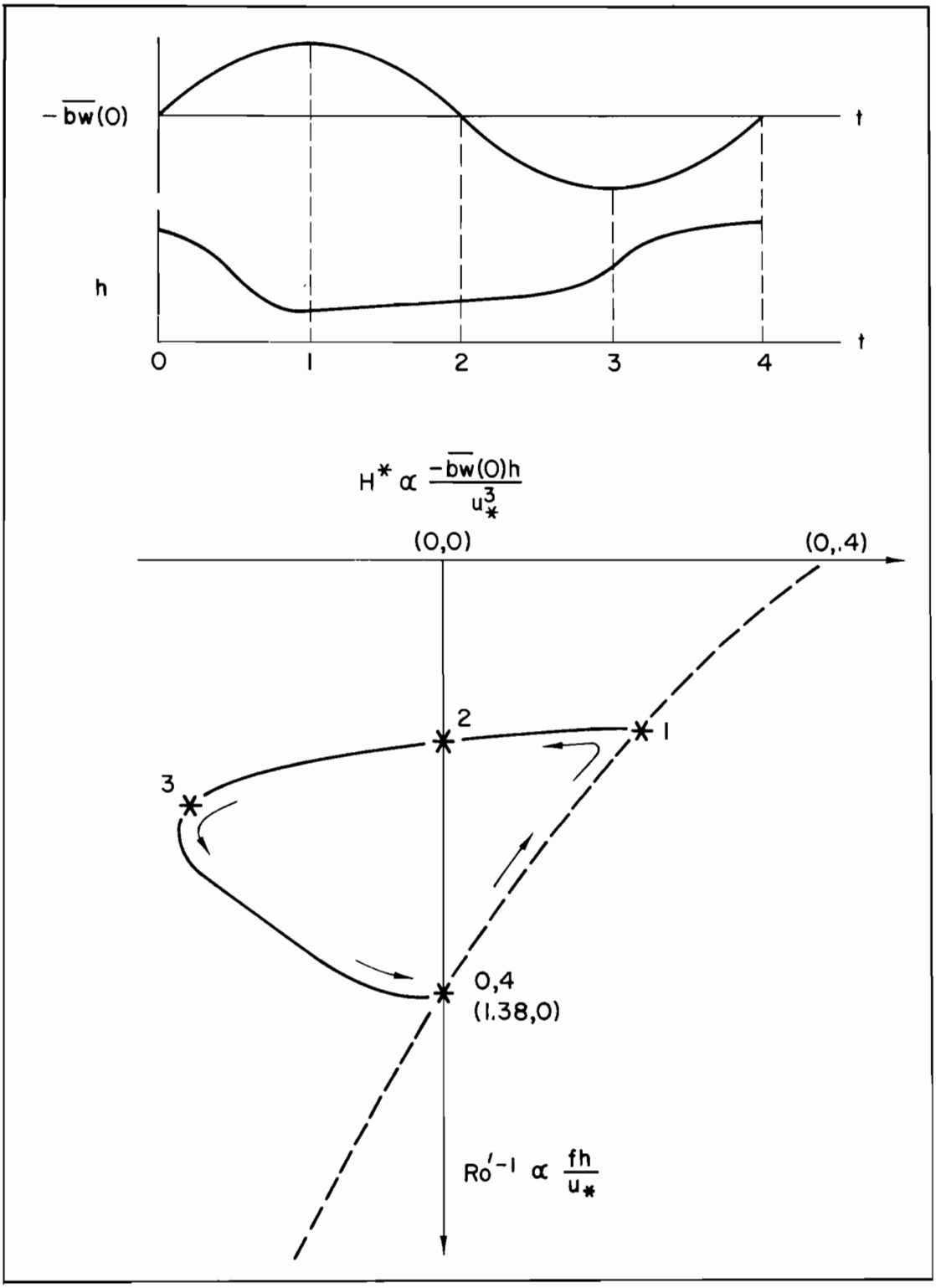

Figure 15. Cyclical steady state in the (H^*, Ro^{-1}) plane.

after [3] erosion of the thermocline is enhanced by both increased system potential energy and by buoyant production which remains strong even though $(\overline{bw})$ is decreasing.

Of course, the real oceanic system is not in an exactly repeating annual cycle. However, year-to-year variations resulting in long-term changes in heat storage can be predicted accurately only by a model that can simulate the hypothetical cyclical steady-state. Any net annual buoyancy flux across the surface that is balanced by advection is not of concern in studying the model in the one-dimensional form. In any case, a large seasonal variation in $\overline{bw}(0)$--and u_*^2--and the resultant cyclical response are dependent upon the proper model response for the more simple situation.

6.3 Simple Hypothetical Cases Demonstrating the Behavior of the Solution

6.3.1 Shallow or $f \simeq 0$ (Ro >> 1).

(1) Initial linear stratification

(a) $\overline{bw} = 0$, $u_*^2 = \text{constant}$

The result is the same as that predicted by the Kraus-Turner type model as well as by the Kato and Phillips experiment. See Figures 16 and 17.

$$\frac{dh}{dt} \propto \frac{u_*^3}{h\Delta B}$$

giving

$$h \propto t^{1/3} .$$

The reason these models are in agreement is that with $b_* = 0$, u_* is the only turbulent velocity scale.

$$\langle \overline{w^2} \rangle \propto \langle \overline{E} \rangle \propto u_*^2 .$$

(b) Free convection: $\overline{bw}(0) = \text{constant} > 0$, $u_*^2 = 0$.

This situation is out of range for Figure 13 because $H^* \to -\infty$. However, if the model equations are nondimensionalized on the buoyancy flux velocity scale $(u_* b_* h)^{1/3}$, rather than on (u_*), the problem may be solved. In this case, $h \propto t^{1/2}$, which is also in agreement with the Kraus-Turner type models.

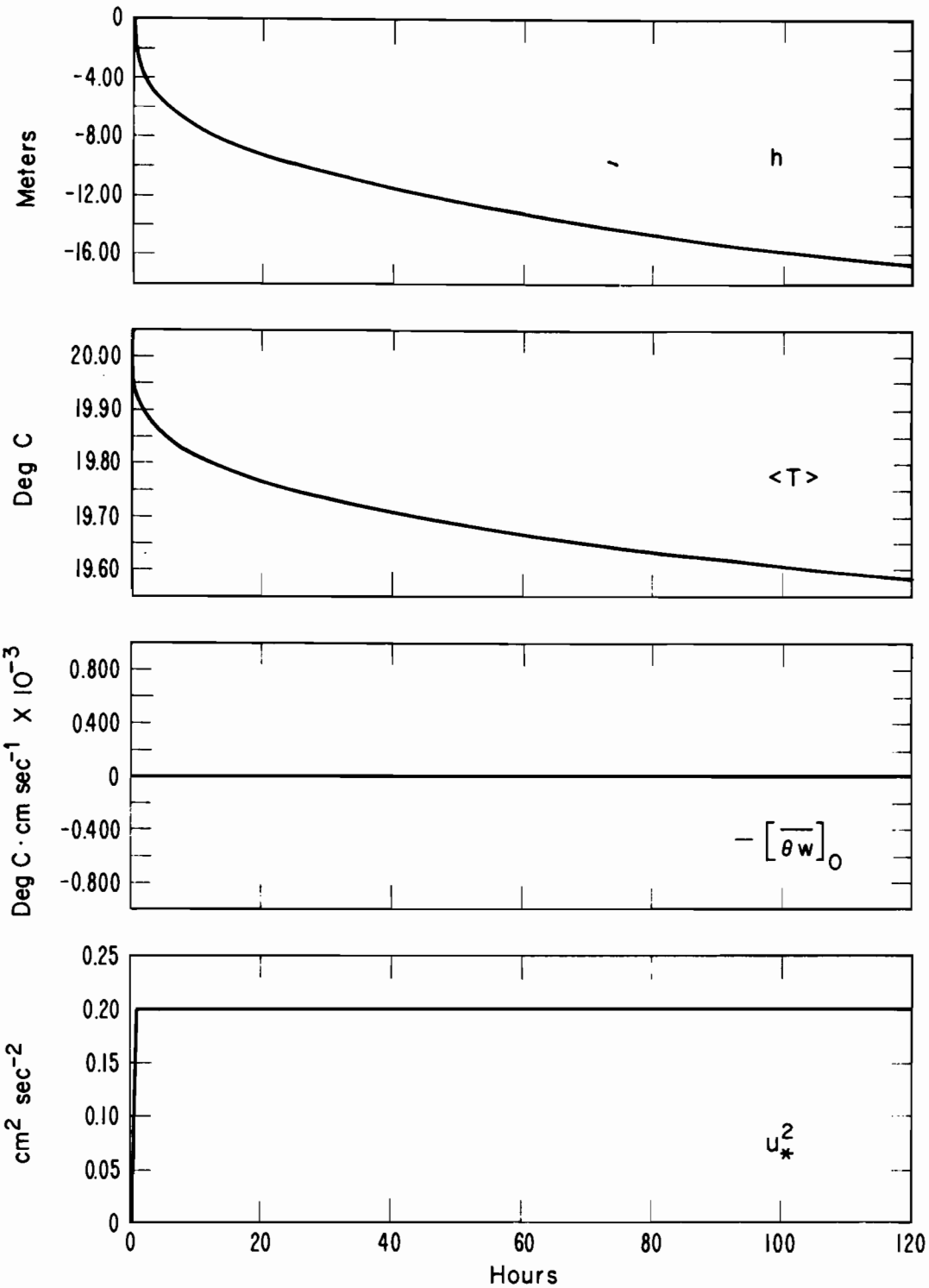

Figure 16. Solution to h(t) for case with initial linear stratification; $\overline{b'w'}(0)=0, u_*^2$ = constant.

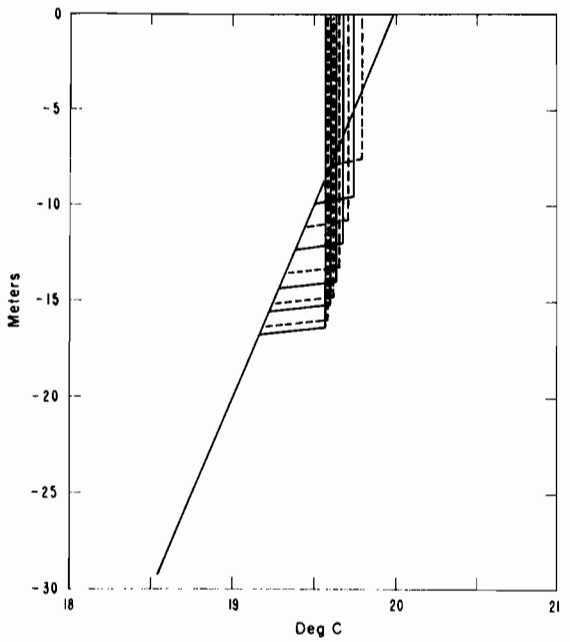

Figure 17. Temperature profile at 12-hour intervals for five days, starting with an initial linear stratification. There is no surface heat flux and a constant wind stress is imposed at time zero.

(c) Cyclical surface buoyancy flux: $\overline{bw}(0) \propto \sin wt$, u_*^2 = constant.

Figures 18 and 19 show the response of the mixed layer to a simple hypothetical diurnal heating and cooling cycle. The magnitude of the heat flux was chosen to be particularly large in order to accentuate the features in a relatively short time span. The initial stratification is the same as for the earlier neutral ($\overline{bw}(0) = 0$)run, 1°C/20m. The wind stress is also the same, 0.2 dynes.

Over the five-day period there is an overall cooling trend because of the entrainment process and lack of net surface heat flux. However, the daily maximum surface temperature is greater than the initial surface temperature for all five days.

Starting with the fourth day, there is larger retreat corresponding to the decrease in the Obukhov length scale relative to the value of h. In spite of midday retreat, the mixed layer more than recovers the temporarily decreased vertical extent. Without eventual enhancement of dissipation, deepening would continue without bound.

A comparison between Figures 18 and 16 demonstrates another important difference, in addition to the presence of a strong diurnal layer temperature change. Although there is no net surface buoyancy flux for either case, the situation having the diurnal cycle has a distinctly slower average rate of deepening. This holds even for the first three days when there is no retreat.

The explanation for this phenomenon lies in the nonlinearity of P* (H*) (Figure 12).

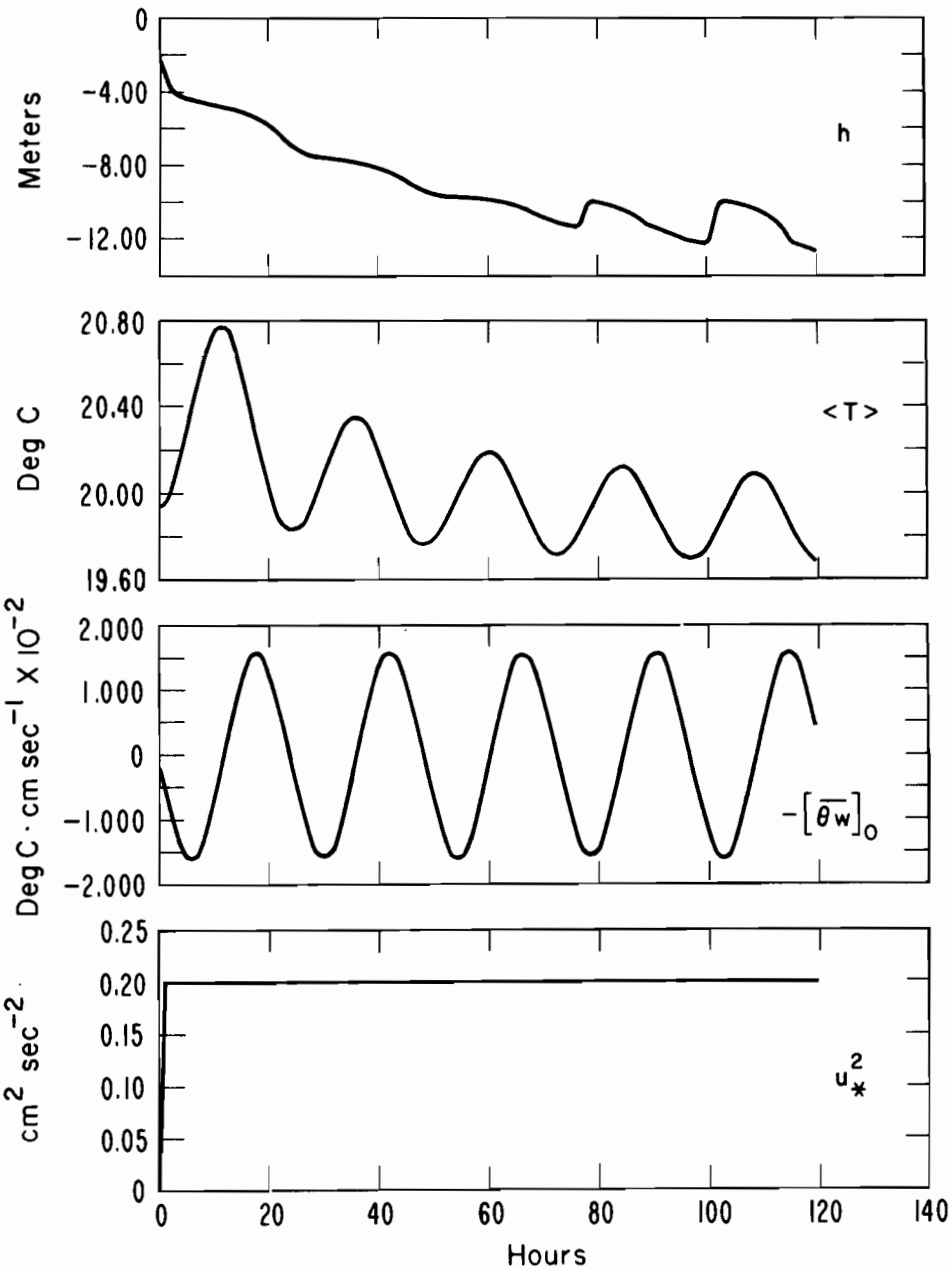

Figure 18. Solution to h(t) for case with cyclical surface heat flux; $\overline{\theta w}(0) = 0.015 \sin(\omega t)$. Compare with Figure 16.

(d) General: $u_*^2 \neq 0$, $\overline{bw}(0) \neq 0$

Since the earlier model projects a linear P*(H*), only two points (at two values of H*) may be made to agree with this model. For example, if summer "retreat" and the neutral ($\overline{bw}(0) = 0$) cases are coincident in both models, then the winter deepening rate will be greater for the earlier model. This is the mathematical difference in the basic responses.

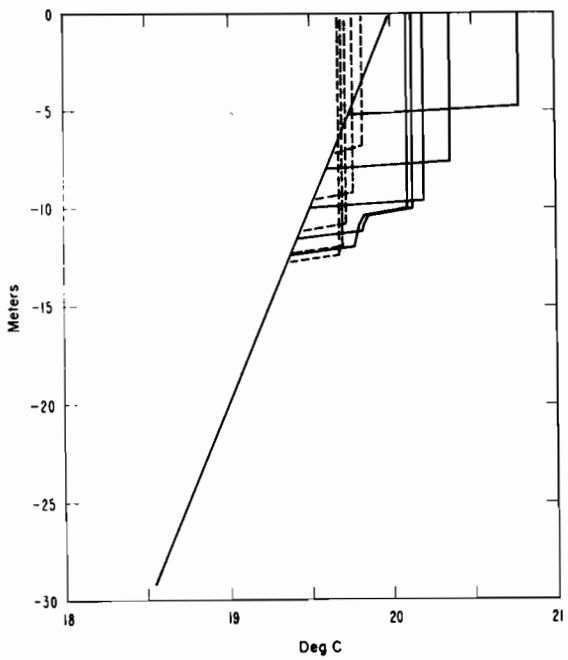

Figure 19. Temperature profile for case with initial linear stratification, with cyclical surface heat flux. Compare with Figure 17.

The physical difference may best be seen from the Tennekes (1973) model in which

$$-\overline{bw}\Big]_{-h} \propto \frac{\langle\overline{E}\rangle^{3/2}}{h}$$

and

$$\langle\overline{E}\rangle^{3/2} \propto m\, u_*^3 - u_* b_* h \ .$$

This model is identical in response to the Kraus-Turner model and is suitable for comparison here because it identifies the turbulent velocity scale $\sqrt{\langle\overline{E}\rangle}$. Then retreat ($dh/dt < 0$) can occur only when $\langle\overline{E}\rangle \to 0$!

Tennekes did not intend for this formula to be extrapolated to the strongly stable situation. Instead, he suggested it as an interpolation between the neutral and free convection cases--the typical atmospheric boundary layer range. Nevertheless, the above is equivalent to recent oceanic applications of the Kraus-Turner type model. The particular problem with applying this method to the stable, retreating mixed layer is that there must still be significant turbulent energy ($\langle\overline{E}\rangle > 0$) above $z = -h_r$. Consequently, the fraction of turbulent energy going to increase the potential energy cannot be independent of stability, H*. This explains the curvature of P*(H*) and the slower rate of damping for the hypothetical case with an oscillating surface buoyancy flux.

(2) Cyclical surface buoyancy flux

No 1-D steady state is achievable because for $f = 0$, h can be limited only by the Obukhov length scale, therefore requiring a net downward buoyancy flux (or heating). Then $\overline{bw}(0)$ could be balanced only by advection. Gill and Niiler (1973) have shown that advection is insufficient for latitudes greater than about 15°.

6.3.2 Convective planetary boundary layer with order one Rossby number

(1) Neutral steady state

With zero surface heat flux, a steady state is predicted (see Fig. 14 at the limit $h \to 1.38\ u_*/f$). Starting from an initial linear stratification and $h < u_*/f$, steady state would be approached only after a relatively long time. This is not likely to be achieved in geophysical flows, except perhaps by the atmospheric boundary layer during the polar winter. See Businger and Arya (1974).

(2) Cyclical steady state

This situation has already been qualitatively described and illustrated by Figure 15, but the relative importance of the rotational and surface buoyancy flux scales needs to be estimated.

For the sake of studying the relative response of the mixed layer, all cycles will be assumed to be repetitive (in steady state). A sinusoidal surface buoyancy flux and a constant wind stress are used to drive the model.

$$\tau = \rho_0 u_*^2 .$$

$$\overline{bw}(0) = - |\overline{bw}(0)| \sin \omega t .$$

The layer response is found to be a function of the parameter B*, the ratio of the buoyancy flux scale to the rotational scale.

$$B^* = \frac{|\overline{bw}(0)|}{f u_*^2} . \qquad (6.10)$$

Figure 20 shows the cycle of $h(t)$, nondimensionalized on u_*/f as a function of B*.

For large B*, which is typical of the annual cycle for temperate oceanic regions, the low minimum mixed layer depth at $\omega t = \pi/2$ is attributable to the strong influence of the buoyant damping corresponding to a small positive Obukhov length scale.

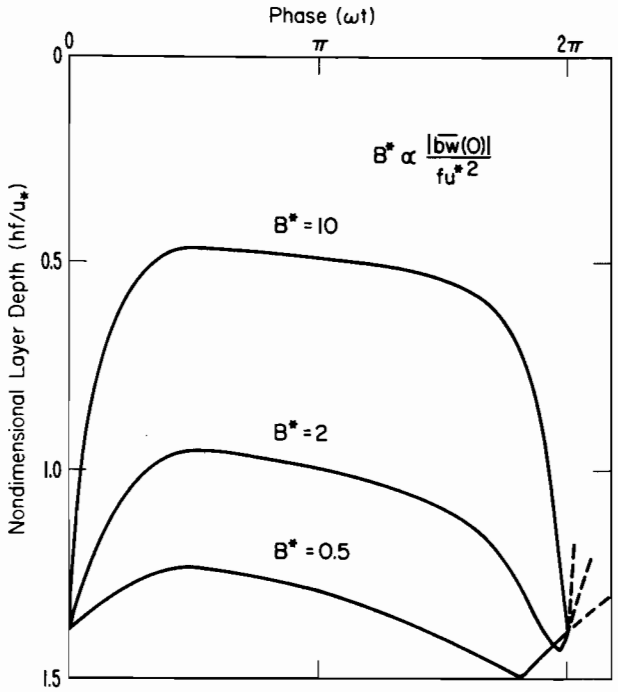

Figure 20. Cyclical steady-state mixed-layer response to sinusoidal surface buoyancy flux and constant wind stress. $\tau=\rho_0 u_*^2$; $\overline{bw}(0)=-|\overline{bw}(0)|\sin(\omega t)$.

In addition to the change in the range of h with B*, there is an important change in the shape of the function h(t). For the case of weak heating and cooling, the variation in h is almost in phase with $\overline{bw}(0)$. In the H* - Ro^{-1} plane (Fig. 21), the locus of the cycle would be small and elongated. For increasingly larger B*, the heat and therefore buoyancy is stored during the "summer" at an increasingly shallower depth (in comparison with $h_{max} \sim u_*/f$). This creates a substantial potential energy deficit which

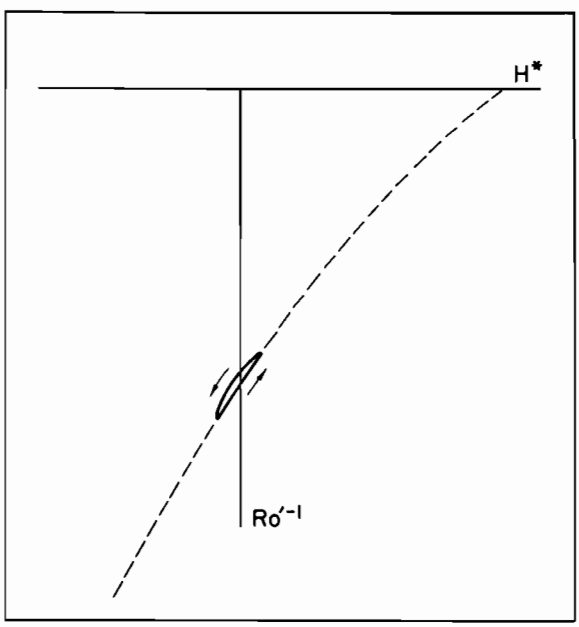

Figure 21. Cyclical steady-state in the (H^*, Ro^{-1}) plane for very small cyclical surface buoyancy flux ($B^*<<1$).

results in a hysteresis effect by retarding the entrainment process. This phase lag in the heat storage naturally has important implications for the interaction with the atmosphere for all cyclical time scales--from one day to periods of climatological importance.

(3) Fluctuations in wind stress: storms

Fluctuations in the wind stress, particularly in the instance of storms, are very important in the annual evolution of the mixed layer and the heat storage of the upper ocean.

Running the model for a simulated annual heating/cooling cycle as before, but adding periodic "storm" pulses of wind stress gives qualitatively little apparent change in h(t). (see Fig. 22). However, the spikes in the retreat side caused by the storms greatly enhance the storage of heat at depth. The midsummer profile (Fig. 23) with the step-like remnants of earlier storms, has an overall potential energy significantly greater than would be the case with no storms. This, in turn, will tend to enhance the eventual deepening, countering to some degree the hysteresis of the heat storage in the annual cycle. The annual range of surface temperatures (see Fig. 24) is less than it would be without storms because of the increased heat storage at depth.

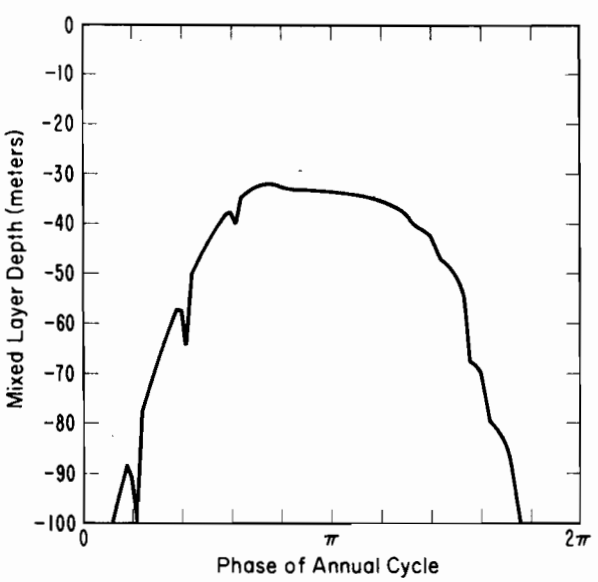

Figure 22. Mixed layer depth h(t) for hypothetical annual cycle including storms: Case A; model without diurnal cycle.

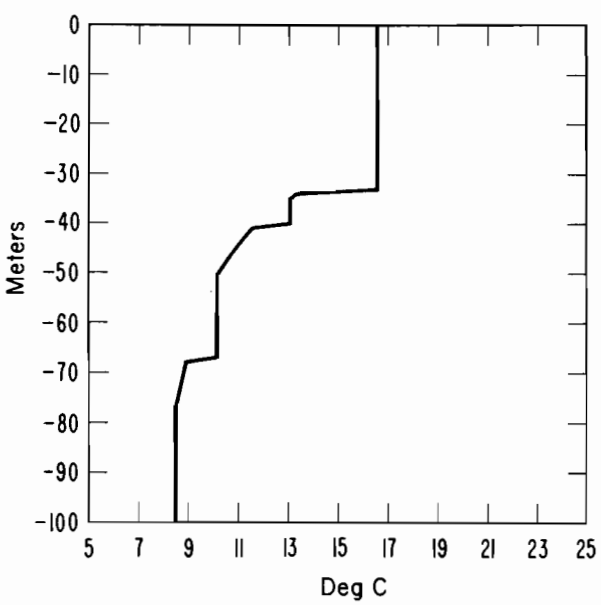

Figure 23. Midsummer temperature profile for case A, model without diurnal cycle.

6.4 Filtering Effect of the Storage of Turbulent Kinetic Energy

The hypothetical solutions shown in Figure 20 are all for periods $(2\pi/\omega)$ much longer then the integral time scale of the turbulence, governed by the dissipation time scale (τ_ε). This made possible the assumption of quasi-steady state so that the turbulent energy storage terms, $\partial/\partial t \langle u_i u_i \rangle$, could be neglected in the solutions. However, fluctuations in the surface boundary conditions u_*^2 and $\overline{bw}(0)$ of sufficiently short period require the consideration of these terms.

A very simple model, which may be solved analytically, provides the answers to the question concerning the importance of this unsteadiness and how it might be treated.

In the simple model only the two largest terms, shear production and dissipation, are balanced by the time rate of change of the turbulent kinetic energy.

$$\frac{\partial \langle \overline{E} \rangle}{\partial t} + \frac{\langle \overline{E} \rangle}{\tau_\varepsilon} = \frac{u_*^3}{h} (1 + a \sin \omega t) \qquad (6.11)$$

The prescribed shear production is a constant plus a sinusoidally-varying component ($a < 1$). By defining dimensionless time,

$$\tau^* = t/\tau_\varepsilon \ , \qquad (6.12)$$

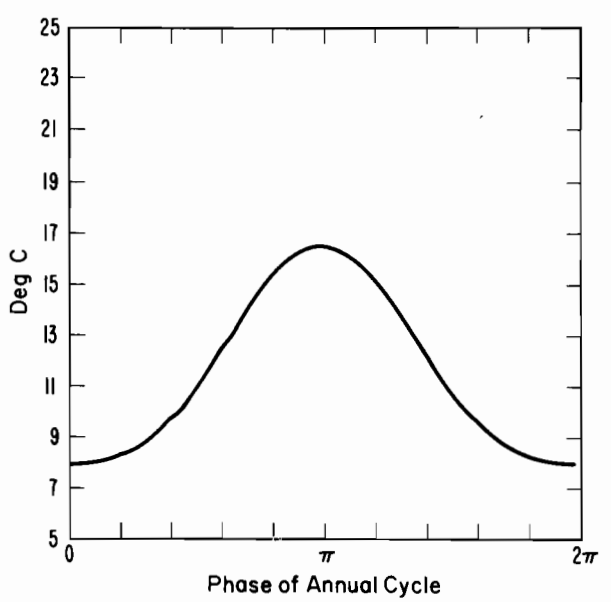

Figure 24. Surface temperature T(z=0,t) for the hypothetical case with storms: Case A, model without diurnal cycle.

and turbulent energy,

$$\Psi^* = \frac{h\langle\overline{E}\rangle}{u_*^3 \tau_\varepsilon} , \tag{6.13}$$

(6.11) is transformed to (6.14),

$$\frac{\partial \Psi^*}{\partial \tau^*} + \Psi^* = 1 + a \sin \omega^* \tau^*, \tag{6.14}$$

where

$$\omega^* = \tau_\varepsilon \omega. \tag{6.15}$$

For (a = 0) the steady-state solution is simply $\Psi^* = 1$. For finite (a), the complete solution, neglecting the initial transient, is

$$\Psi^* = 1 + \left(\frac{a}{\omega^{*2} + 1} \right) (\sin \omega^* \tau^* - \omega^* \cos \omega^* \tau^*) . \tag{6.16}$$

There is a phase shift that increases with (ω^*), but the important aspect of (6.16) is the relative magnitude of the response associated with the fluctuating component. Figure 25 is a plot of this versus ω^*.

For $\omega^* < \sim 0.5$ (slow fluctuation period compared with τ_ε), the situation of quasi-steady state is satisfied. Depending upon the Rossby number and H*, this corresponds to a minimum fluctuation period of several hours up to about a day.

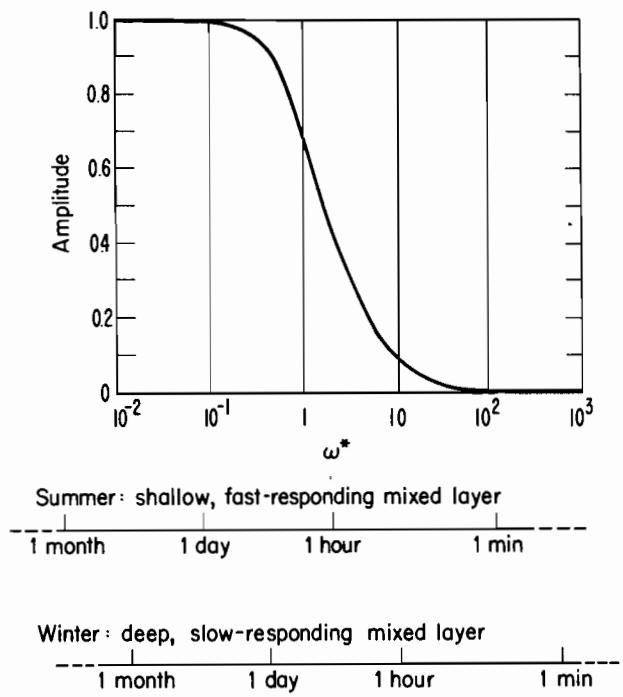

Figure 25. Response of the mixed layer to fluctuations in the surface boundary conditions: filtering effect.

For faster fluctuation having a period less than about an hour, the phase shift (lag) in the response approaches 90° and, most importantly, the amplitude of the response is negligible. In other words, the high frequencies are filtered out.

This becomes a possible cause of error in using observed winds to drive a model having an integration time step smaller or comparable with τ_ε. If the quasi-steady state assumption is made to facilitate solution, but the surface boundary conditions are not properly smoothed or filtered, an incorrect high-frequency response will not only be present but will bias the mean trend.

6.5 Interaction Between Forcing Time Scales: Modulation of the Longer-Period Trend in the Diurnal-Period Heating/Cooling Cycle

As already shown in comparing Figure 18 with Figure 16, if H* is perturbed by a diurnal-period heating cycle, then the mean P* over the cycle will be less than P* of the mean H*.

$$\overline{P^*\,(H^*)} < P^*\,\overline{(H^*)}\ . \qquad (6.17)$$

An atypical situation was used in Figure 18 to demonstrate the effect of (6.17) during a relatively short time period. Over a year, however, the consequences can be significant. This is shown by Figures 26-28--case "B." Case "B" is the same as case "A," Figures 22-24, except for the superposition of a diurnal cycle on top of the annual heating/cooling cycle.

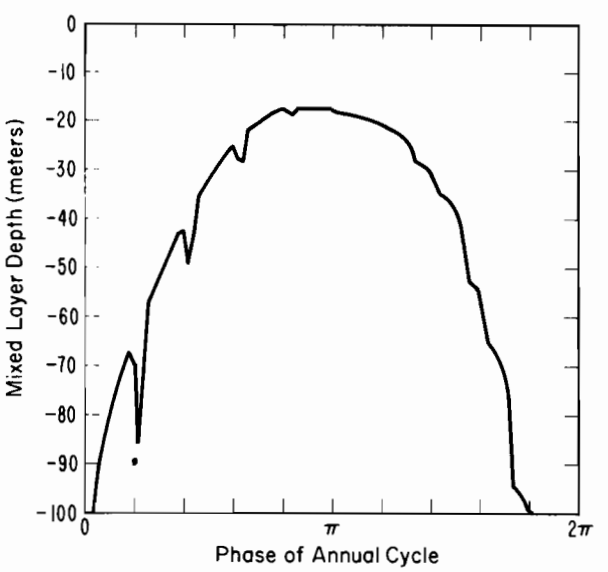

Figure 26. Mixed layer depth h(t) for hypothetical annual cycle, Case B: model with diurnal heat flux cycle (compare with fig. 22).

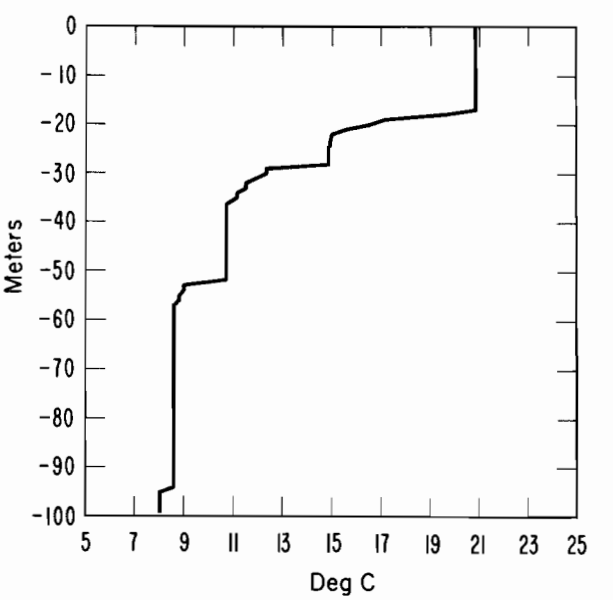

Figure 27. Midsummer temperature profile, case B: Model with diurnal cycle. (Compare with fig. 23).

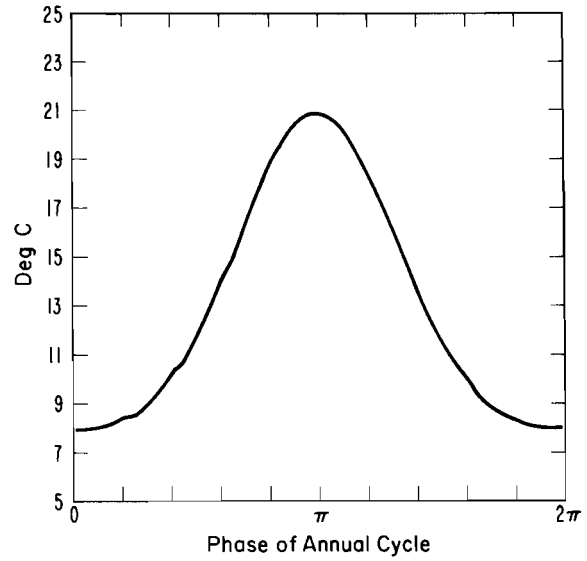

Figure 28. Surface temperature, case B: Model with diurnal cycle (compare with fig. 24).

Throughout the year, the principal effect is the decrease in mixed layer depth. The decrease in upper ocean potential energy, higher surface temperatures, and lower heat storage at depth are directly due to the modulation of the longer-term entrainment rate.

The basic shapes of the two solutions to h(t) are similar. Without a noticeable difference in phase, there is the possibility that the effect may be absorbed in the constants of calibration. In other words, a one-day or longer time step might be possible if computation speed were of the essence in a numerical model.

6.6 Simulation of a Real Case

An experiment conducted by Halpern (1974) provides a unique record of 1-D mixed layer evolution in that wind, currents, and thermistor chain measurements were made simultaneously at one location (47°N, 128°W) for the period of a month. During this time one "strong" and several lesser storm events occurred. Figures 29-33 show the model results.

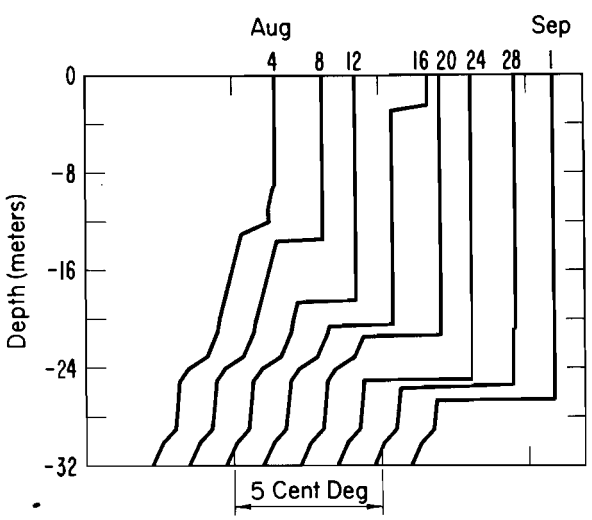

Figure 29. Sequence of temperature profiles predicted by the model (Successive profiles offset by 1.25 degrees).

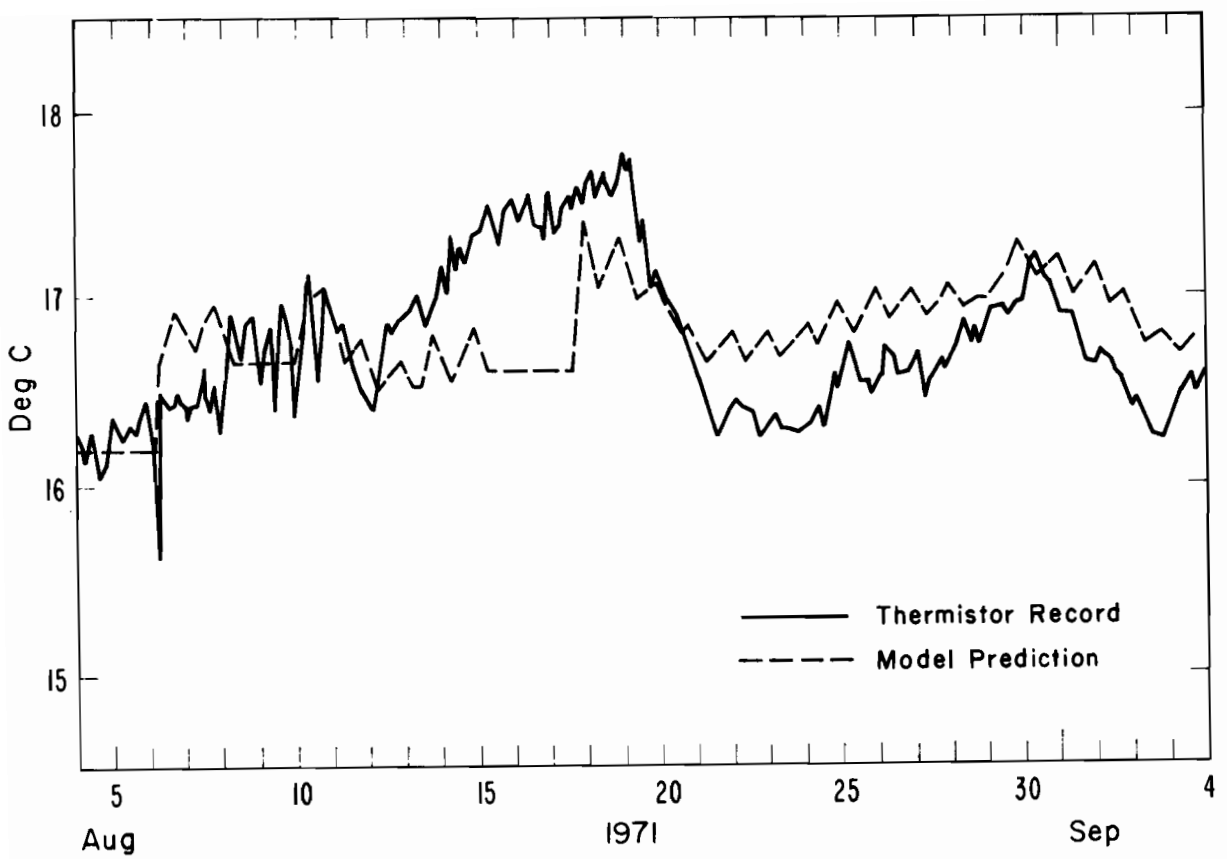

Figure 30. Comparison between observed and predicted temperatures at 9.6-meter depth.

Here the 31-day records of temperature at 9.6 and 23.4 meters are compared with the model prediction. The actual wind speeds are used to compute u_*^2 for the model, but surface buoyancy flux is rather crudely assumed to be constant plus a constant-amplitude diurnal component. Nevertheless, the gross features of the record are reproduced:

(1) A weak storm on August 11 deepens the layer from 13 to 18 meters.

(2) A period of low winds from August 13 to August 19 resulted in a retreating layer and warming at the 9.6-meter depth. During this period the guessed-at surface heat flux gave a too-shallow depth of retreat that can be seen in the August 16 temperature profile. Therefore the predicted temperature at 9.6 meters is too low until the layer deepens sufficiently on August 17.

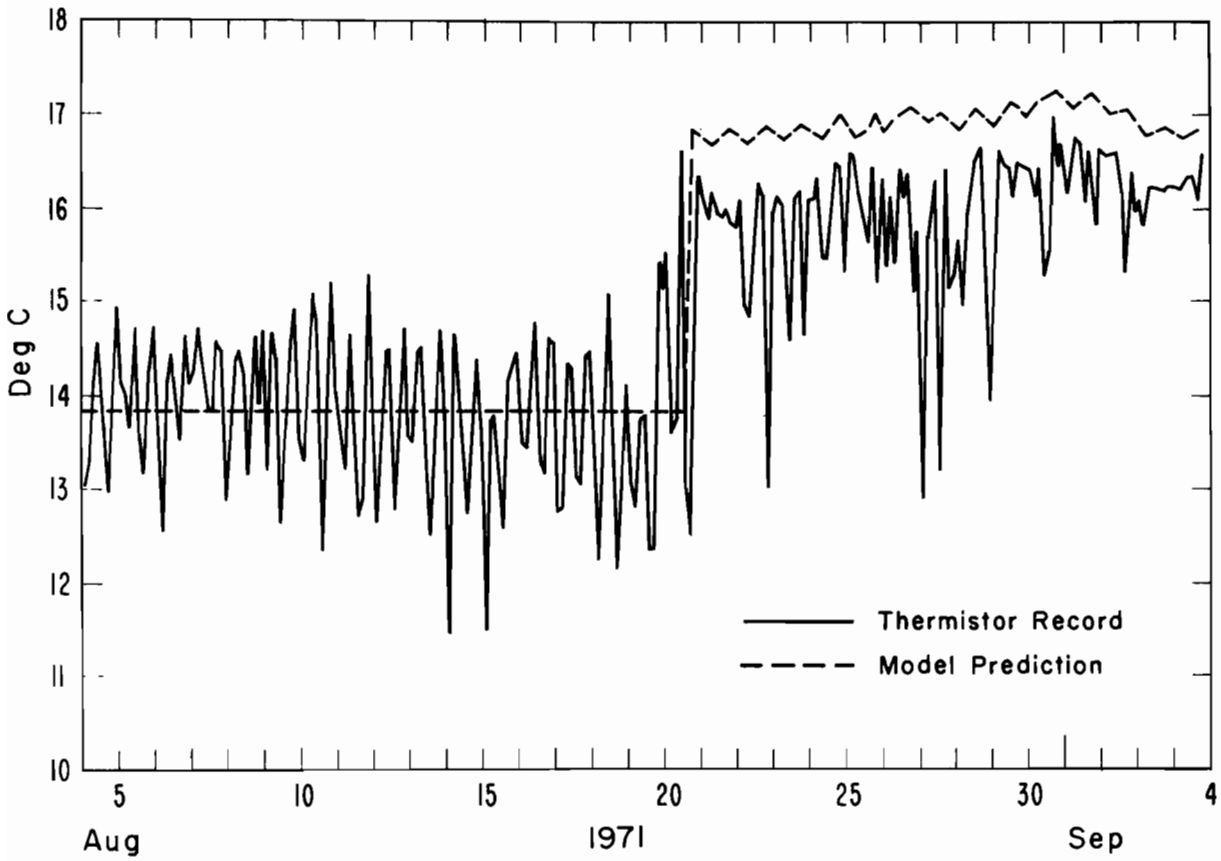

Figure 31. Comparison between observed and predicted temperatures at 23.4-meter depth.

(3) The relatively strong storm of August 20 deepens the layer to over 24 meters and the temperature at 9.6 meters drops considerably. At this time the 23.4-meter thermistor for the first time lies within the mixed layer and registers the higher temperature.

(4) Subsequent warming and then cooling after August 30 is due to another storm. This last storm is nearly as strong as that of August 20, but its work is not as obvious because it starts with a relatively deep layer.

Figure 32 shows another possible model output--the mixed layer wind-driven current. As shown by Figure 12, the mean current at the base of the mixed layer has only a small effect upon the turbulent energy budget (even for $Ri^* \sim 1$). The depth of the mixed layer, on the other hand, directly influences the amplitude of C. Therefore, any surface current prediction requires knowledge of h(t).

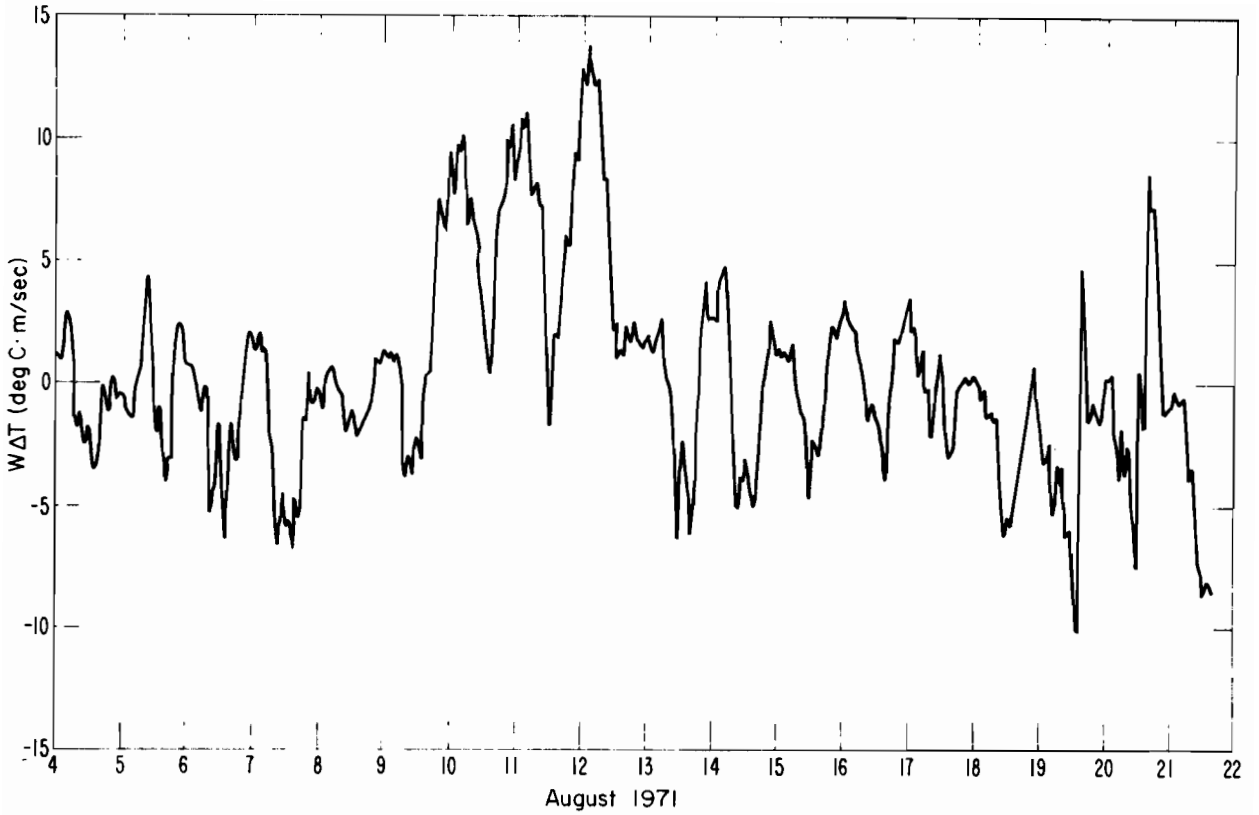

Figure 32. A measure of sensible heat flux at the ocean surface by buoy observations (courtesy of David Halpern). $\overline{\theta w}(0) \propto W\Delta T$; W = wind speed at 2 meters above surface; ΔT = surface water temperature minus air temperature.

6.7 Evaluation of Model Output

This simulation of a real case is not a strict test of the model. The surface buoyancy flux is not known sufficiently well for this run to be used either for calibration purposes or as a test of model behavior.

Inasmuch as the model was designed to have general applicability over all seasons (wide range of values for H*), the proper calibration and testing procedure requires an integration over a full year. This remains to be done at a future date under a more operationally-oriented program of research.

Figure 32 shows a measure of the sensible heat flux at the surface (by a bulk parameterization) versus time for the first half of the total period of observation. (Air temperature was not available after the storm of 21 August.) Because relative humidity was not available, the relatively larger latent heat flux could not be computed. Because the latent heat flux is very roughly proportional to the sensible heat flux (assuming an approximately constant Bowen ratio), Figure 32 indicates the large magnitude of the net

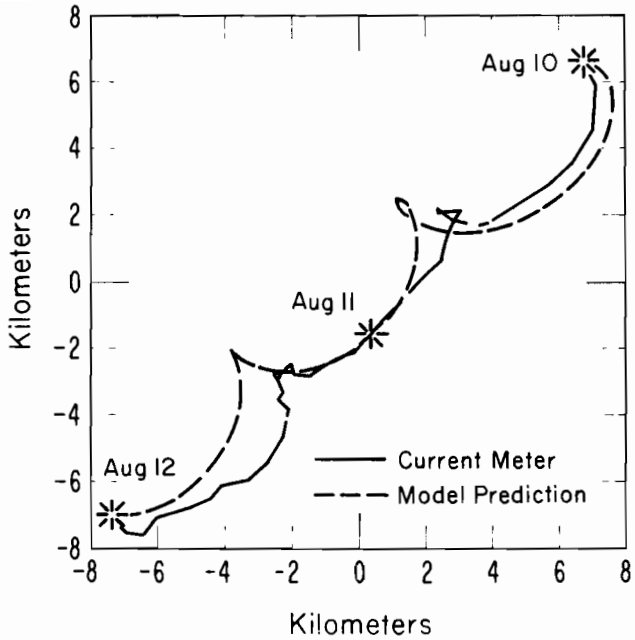

Figure 33. Measured and predicted progessive vector diagrams of current at 8.3 meters for two days of the Halpern observations.

diurnal heat flux compared with the mean daily values. The mean daily heat flux and the diurnal component were assumed to be constant over the entire period. This was obviously not true.

Nevertheless, this particular run, as illustrated by Figures 29 to 33, does have didactic value in demonstrating the character of the model response to realistic boundary conditions. The overall conclusion for this particular case is that the wind stress controls the timing of the entrainment and retreat events. The degree of surface heating or cooling is important in determining the extent of the retreat or the deepening. Although the guess at $\overline{bw}(t)$ was only marginally satisfactory, an important result is that the diurnal cycle prescribed gives a much better prediction than does an integration using a constant heat flux alone.

7. CONCLUSIONS

This model for the ocean mixed layer consists of a number of hypotheses and assumptions regarding the mechanical energy budget, originally shown in Figure 1. In arriving at these hypotheses, mean turbulent field techniques were used, but this was done without losing the simplicity of the bulk model concept. The particular details of the structure of the mean fields within the boundary layer were not of highest priority as a model output. In any case detailed geophysical data revealing this structure is unavailable to test such a prediction. Of highest importance in this model was the ability to predict the year-round evolution of the ocean mixed layer depth, together with the bulk properties. There are several models, including those by Wyngaard et al. (1974) and Sundararajan (1975), which provide structural predictions quite nicely, but these boundary layer models are not directly

concerned with a changing layer height. An entrainment model is necessary to provide boundary conditions at the moving density interface.

The atmospheric and oceanic boundary layers present nearly identical problems. However, an important difference arises in the surface heat flux boundary condition. The atmospheric boundary layer is predominantly unstable because of minimal absorption of solar radiation within the layer. On the other hand, most of the solar radiation is absorbed near the ocean surface and hence turbulent heat flux downward in the oceanic boundary layer is about the same as flux upward in the course of an annual cycle. Therefore, the stable situation is of relatively greater importance in the ocean. As shown by Figures 12 and 14, the nonlinearity of P^* (H^*) is greatest for $H^* > 0$, the stable region. The treatment of the oceanic case must be made with emphasis upon this point since the linear extrapolation of the unstable situation will not suffice.

In addition to the nonlinear dependence upon stability, a Rossby number dependence for the entrainment rate has been found in the nondimensional solution, Figure 14. This makes possible a cyclical steady state for the boundary layer without resorting to unrealistic values of upwelling or lateral advection in a long-term integration.

In the short term, on the order of days, the upper ocean, even at higher latitudes, exhibits significant three-dimensional baroclinic activity. A case in point is well documented by Gregg (1975) in which only lateral advection can explain the change in heat content after the passage of a storm. In doing the ensemble or horizontal averaging, such phenomena as well as the short-period internal waves are treated as noise in the essentially one-dimensional mixed layer dominated by the strong vertical turbulent fluxes of heat, salt, and momentum. This does not eliminate the practical difficulties of analyzing and simulating actual observations made at a single point, as shown by the case using real winds to drive the model.

The importance of shorter-period fluctuations in the surface buoyancy flux in modulating the longer-term response has demonstrated the need to know the typical daily heating/cooling cycle: Solar radiation, evaporation, conduction, and back-radiation as a function of season and geographical coordinates. The detailed features of this diurnal cycle were not of importance in conducting a qualitative evaluation, but accurate quantitative results from an operational model would be impossible without them. For the same reason, the radiation absorption function should be known. This last suggestion may not be possible without the incorporation of a primary productivity model in which case the physics becomes directly dependent upon the biology!

Some of the most fruitful applications of this model lie in the link-up with other models. The region below the mixed layer has been over a short time period successfully treated as a zero-flux "quiescent abyss." This was done primarily for simplicity when the point of focus was the overlying turbulent boundary layer. The first natural joining of models is between such a boundary layer model with an ocean general circulation model. But why stop there? An atmospheric general circulation model may be combined with

the ocean general circulation model--but only through two boundary layer or mixed layer models. It has been demonstrated here that the sea-surface temperature, which is so important for weather prediction, cannot be predicted with accuracy without the proper consideration of the ocean mixed layer. Climate modeling must also pay heed to the oceanic boundary layer. Anomalous events in the evolution of the mixed layer may induce a delayed response by the atmosphere when the mixed layer again deepens sufficiently.

The interaction between diurnal and annual time scale events has been particularly emphasized, but other time scales even longer than a year pose some interesting possibilities, particularly for inactive models.

8. SUMMARY OF MODELED EQUATIONS

ENTRAINMENT BUOYANCY FLUX

$$-\overline{bw}\,(-h) = \frac{m_4 \,\langle \overline{w^2} \rangle^{\frac{1}{2}} \,\langle E \rangle}{h} \tag{1}$$

BUDGET FOR HORIZ. COMPONENTS OF TURB. KINETIC ENERGY

$$\frac{1}{2}\frac{d}{dt}\left(h\,\langle \overline{u^2 + v^2} \rangle\right) = m_3\, u_*^3 - \frac{h\,\overline{bw}\,(-h)}{2\,Ri^*} \tag{2}$$

$$-m_2\,(\langle \overline{E} \rangle - 3\,\langle \overline{w^2} \rangle)\;\langle \overline{E} \rangle^{\frac{1}{2}} - \frac{2m_1}{3}\left(\langle \overline{E} \rangle^{\frac{1}{2}} + fh\right)\langle \overline{E} \rangle$$

BUDGET FOR VERTICAL COMPONENT OF TURB. KINETIC ENERGY

$$\frac{1}{2}\frac{d}{dt}\left(h\,\langle \overline{w^2} \rangle\right) = \frac{\dot{h}\,\overline{bw}(-h)}{2} + \frac{h\,\overline{bw}(0)}{2} \tag{3}$$

$$+ m_2\,(\langle \overline{E} \rangle - 3\,\langle \overline{w^2} \rangle)\,\langle \overline{E} \rangle^{\frac{1}{2}} - \frac{m_1}{3}\left(\langle \overline{E} \rangle^{\frac{1}{2}} + fh\right)\langle \overline{E} \rangle$$

CONSERVATION OF MEAN BUOYANCY AND MEAN MOMENTUM

$$h\,\frac{d\,\langle B \rangle}{dt} = \overline{bw}\,(-h) - \overline{bw}\,(0) + \frac{\beta g}{\rho_0 C_p}\int_{-h}^{0} Q\,dz \tag{4}$$

$$h \frac{d \langle C \rangle}{dt} = \overline{cw}\,(-h) - \overline{cw}\,(0) - \text{if } \langle C \rangle\, h \qquad (5)$$

"JUMP CONDITIONS" AT BOTTOM OF MIXED LAYER

$$-\overline{cw}\,(-h) = \Delta C \frac{dh}{dt}$$

$$-\overline{bw}\,(-h) = \Delta B \frac{dh}{dt}$$

NOTATION

$C = U + i\,V$

$E = u^2 + v^2 + w^2$

$u_*^2 = |\overline{cw}\,(0)|$

$B = (\rho_0 - \overline{\rho})\, g/\rho_0$

$\beta = \rho_0^{-1}\, \partial\rho/\partial T$

$$Ri^* = \frac{h\Delta B}{|\Delta C|^2}$$

$$(\overline{\ }) = \lim_{L\to\infty} \frac{1}{L^2} \int_{-L/2}^{L/2} \int_{-L/2}^{L/2} (\ )\, dxdy$$

$$\langle (\ ) \rangle = \frac{1}{h} \int_{-h}^{0} (\ )\, dz$$

9. ACKNOWLEDGMENTS

This dissertation and the research leading to it were accomplished with the assistance and encouragement of many.

Dr. David Halpern, as Chairman of the Supervisory Committee, provided support and advice in a manner that permitted the evolution of this work in a most creative atmosphere.

Professors Joost Businger and Frank Badgley, in addition to participating on the Reading Committee, helped lay the foundation of my understanding of turbulent boundary layers. As a visiting professor, Dr. John Wyngaard introduced me to the techniques of mean-turbulent-field modeling.

Dr. Eric Kraus, by inviting me to participate in the N.A.T.O. Advanced Study Institute at Urbino in September 1975, gave me the benefit of his own insight as well as that of other primary workers in the field at a most opportune time in the development of this work. Drs. Pearn Niiler and Raymond Pollard were among this group.

Mr. Francis Way must be mentioned because it was he who initially steered my interests toward the ocean.

My parents, Roland William and Geraldine Patrick Garwood, have lent their support for the longest time. It has been greatly appreciated.

Last, but most of all, thank you to my wife Marilyn. With her support this task was made easier, and the entire period was made to be a most enjoyable one.

10. REFERENCES

Arya, S. P. S., and J. C. Wyngaard (1975): Effect of baroclinicity on wind profiles and the geostrophic drag law for the convective planetary boundary layer. *J. Atmos. Sci.*, 32:767-778.

Benjamin, T. B. (1963): The threefold classification of unstable disturbances in flexible surfaces bounding inviscid flows. *J. Fluid Mech.*, 16:435-450.

Businger, J. A. and S.P.S. Arya (1974): Height of the mixed layer in the stably stratified planetary boundary layer. *Adv. in Geophys.*, 18A, Academic Press, New York, 73-92.

Businger, J. A., J. C. Wyngaard, Y. Izumi, and E. F. Bradley (1971): Flux-profile relationships in the atmospheric surface layer. *J. Atmos. Sci.*, 28:181-189.

Denman, K. L. (1973): A time-dependent model of the upper ocean. *J. Phys. Ocean.*, 3:173-184.

Ekman, V. W. (1905): On the influence of the earth's rotation on ocean currents. *Ark. Mat. Astron. Fys.*, 2(11):1-53.

Farmer, D. M. (1975): Penetrative convection in the absence of mean shear. *Quart. J. R. Met. Soc.*, 101:869-891.

Geisler, J. E. and E. B. Kraus (1969): The well-mixed Ekman boundary layer. *Deep-Sea Res.*, Suppl., 16:73-84.

Gill, A. E. and P. P. Niiler (1973): The theory of seasonal variability in the ocean. *Deep-Sea Res.*, 20:141-177.

Gregg, M. C. (1975): Fine and microstructure observations during the passage of a mild storm. (Unpublished manuscript).

Halpern, D. (1974): Observations of the deepening of the wind-mixed layer in the northeast Pacific Ocean. *J. Phys. Ocean.*, 4 (3): 454-466.

Kantha, L. H. (1975): Turbulent entrainment at the density interface of a two-layer stably stratified fluid system. Department of Earth and Planetary Science Technical Report No. 75-1. Johns Hopkins University, Baltimore, 162 pp.

Kato, H. and O. M. Phillips (1969): On the penetration of a turbulent layer into stratified fluid. *J. Fluid Mech.*, 37:643-655.

Kitaigorodsky, S. A. (1960): On the computation of the thickness of the wind-mixing layer in the ocean. *Bull. Acad. Sci. U.S.S.R., Geophys. Ser.*, 3:284-287.

Kraus, E. B. and C. Rooth (1961): Temperature and steady state vertical heat flux in the ocean surface layers. *Tellus*, 13: 231-238.

Kraus, E. B. and J. S. Turner (1967): A one-dimensional model of the seasonal thermocline, part II. *Tellus*, 19:98-105.

Lamb, H. L. (1932): *Hydrodynamics*. Dover, New York, 738 pp.

Long, R. R. (1974): The influence of shear on mixing across density interfaces. (Unpublished manuscript).

Lumley, J. L. and B. Khajeh-Nouri (1973): Computational modeling of turbulent transport. *Adv. in Geophys.*, 18A, Academic Press, New York, 169-192.

Mellor, G. L. and H. J. Herring (1973): A survey of the mean turbulent field closure models. *AIAA Journal*, 11 (5):590-599.

Miropol'skiy, Yn. A. (1970): Nonstationary model of the wind-convection mixing layer in the ocean. *Izv., Atm. and Ocean Phys.*, 6(12):1284-1294.

Moore, J. M. and R. R. Long (1971): An experimental investigation of turbulent stratified shearing flow. *J. Fluid Mech.*, 49: 635-655.

Munk, W. and E. R. Anderson (1948): Notes on a theory of the thermocline. *J. Mar. Res.*, 7:276-295.

Niiler, P. P. (1975): Deepening of the wind-mixed layer. *J. Mar. Res.*, 33(3):405-422.

Pollard, R. T. and R. C. Millard, Jr. (1970): Comparison between observed and simulated wind-generated inertial oscillations. *Deep-Sea Res.*, 17:813-821.

Pollard, R. T., P. B. Rhines and R. O. R. Y. Thompson (1973): The deepening of the wind-mixed layer. *Geophys. Fluid Dyn.*, 3:381-404.

Rossby, C. G. and R. B. Montgomery (1935): The layer of frictional influence in wind and ocean currents. Papers Phys. Oceanog. and Meteorol., MIT and Woods Hole Oceanogr. Inst., 3 (3):101 pp.

Rotta, J. C. (1951): Statistische Theorie Nichthomogener Turbulenz. *Z. fuer Physik*, 129:547-572.

Sundararajan, A. (1975): Significance of the neutral height scale for the convective, barotropic planetary boundary layer. *J. Atmos. Sci.*, 32(12):2285-2287.

Tennekes, H. and J. L. Lumley (1972): *A First Course in Turbulence*. MIT Press, Cambridge, Mass. 300 pp.

Tennekes, H. (1973): A model for the dynamics of the inversion above a convective boundary layer. *J. Atmos. Sci.*, 30:558-567.

Thompson, R. (1974): Predicting the characteristics of the well-mixed layer. Woods Hole Ocean. Inst. Tech. Report, 76 pp.

Turner, J.S. (1968): The influence of molecular diffusivity on turbulent entrainment across a density interface. *J. Fluid Mech.*, 33:639-656.

Turner, J. S. (1969): A note on wind-mixing at the seasonal thermocline. *Deep-Sea Res.*, 16:Suppl., 297-300.

Wyngaard, J. C., O. R. Coté and K. S. Rao (1974): Modeling of the atmospheric boundary layer. *Adv. in Geophys.* 18A:193-212.

★ U.S. Government Printing Office: 1977-777-045/1225 Region 8